S Army Corps
f Engineers

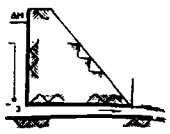

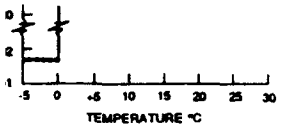

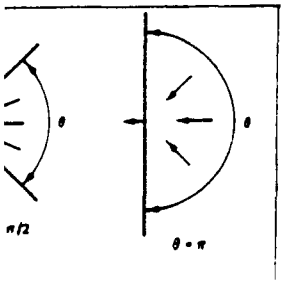

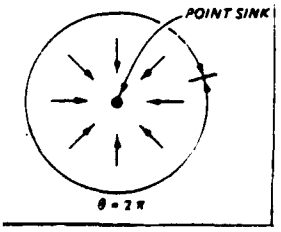

WATER QUALITY RESEARCH PROGRAM

TECHNICAL REPORT W-90-1

SIMULTANEOUS, MULTIPLE-LEVEL WITHDRAWAL FROM A DENSITY STRATIFIED RESERVOIR

by

Stacy E. Howington

Hydraulics Laboratory

DEPARTMENT OF THE ARMY
Waterways Experiment Station, Corps of Engineers
3909 Halls Ferry Road, Vicksburg, Mississippi 39180-6199

November 1990
Final Report

Approved For Public Release; Distribution Unlimited

Prepared for DEPARTMENT OF THE ARMY
US Army Corps of Engineers
Washington, DC 20314-1000

Under WQRP Work Unit 32366

Monitored by Environmental Laboratory
US Army Engineer Waterways Experiment Station
3909 Halls Ferry Road, Vicksburg, Mississippi 39180-6199

Destroy this report when no longer needed. Do not return it to the originator.

The findings in this report are not to be construed as an official Department of the Army position unless so designated by other authorized documents.

The contents of this report are not to be used for advertising, publication, or promotional purposes. Citation of trade names does not constitute an official endorsement or approval of the use of such commercial products.

Unclassified
SECURITY CLASSIFICATION OF THIS PAGE

REPORT DOCUMENTATION PAGE

Form Approved OMB No. 0704-0188

1a. REPORT SECURITY CLASSIFICATION Unclassified	1b. RESTRICTIVE MARKINGS
2a. SECURITY CLASSIFICATION AUTHORITY	3. DISTRIBUTION/AVAILABILITY OF REPORT Approved for public release; distribution unlimited.
2b. DECLASSIFICATION/DOWNGRADING SCHEDULE	
4. PERFORMING ORGANIZATION REPORT NUMBER(S)	5. MONITORING ORGANIZATION REPORT NUMBER(S) Technical Report W-90-1
6a. NAME OF PERFORMING ORGANIZATION USAEWES Hydraulics Laboratory 6b. OFFICE SYMBOL (If applicable) CEWES-HS	7a. NAME OF MONITORING ORGANIZATION USAEWES Environmental Laboratory
6c. ADDRESS (City, State, and ZIP Code) 3909 Halls Ferry Road Vicksburg, MS 39180-6199	7b. ADDRESS (City, State, and ZIP Code) 3909 Halls Ferry Road Vicksburg, MS 39180-6199
8a. NAME OF FUNDING/SPONSORING ORGANIZATION US Army Corps of Engineers 8b. OFFICE SYMBOL (If applicable)	9. PROCUREMENT INSTRUMENT IDENTIFICATION NUMBER
8c. ADDRESS (City, State, and ZIP Code) Washington, DC 20314-1000	10. SOURCE OF FUNDING NUMBERS PROGRAM ELEMENT NO. / PROJECT NO. / TASK NO. / WORK UNIT ACCESSION NO. WQRP 32366
11. TITLE (Include Security Classification) Simultaneous, Multiple-Level Withdrawal from a Density Stratified Reservoir	
12. PERSONAL AUTHOR(S) Howington, Stacy E.	
13a. TYPE OF REPORT Final report 13b. TIME COVERED FROM _____ TO _____	14. DATE OF REPORT (Year, Month, Day) November 1990 15. PAGE COUNT 73
16. SUPPLEMENTARY NOTATION Available from National Technical Information Service, 5285 Port Royal Road, Springfield, VA 22161.	

17. COSATI CODES		
FIELD	GROUP	SUB-GROUP

18. SUBJECT TERMS (Continue on reverse if necessary and identify by block number)

Flow distribution
Intake structures
Reservoir operation
Selective withdrawal
Single wet well
Stratified flow

19. ABSTRACT (Continue on reverse if necessary and identify by block number)

A theory was developed and tested to predict the distribution of flow among multiple ports in a density stratified fluid (e.g., a thermally stratified reservoir). Knowledge of the individual port flows is necessary to accurately estimate the release water characteristics using current selective withdrawal technology. The comparisons between the predictions and observations encompass a wide range of intake structure sizes, port configurations, and flow rates. The comparisons were favorable with the only significant errors limited to an unlikely range of operating conditions.

For a large percentage of potential flows, the resulting stratified-flow-distribution algorithm can predict, with reasonable accuracy, the individual port flows and the desired water quality constituents. This has been incorporated into a subroutine for inclusion in numerical reservoir models.

20. DISTRIBUTION/AVAILABILITY OF ABSTRACT ☒ UNCLASSIFIED/UNLIMITED ☐ SAME AS RPT. ☐ DTIC USERS	21. ABSTRACT SECURITY CLASSIFICATION Unclassified
22a. NAME OF RESPONSIBLE INDIVIDUAL	22b TELEPHONE (Include Area Code) / 22c. OFFICE SYMBOL

DD Form 1473, JUN 86 *Previous editions are obsolete*

SECURITY CLASSIFICATION OF THIS PAGE
Unclassified

PREFACE

This investigation was conducted by the US Army Engineer Waterways Experiment Station (WES), Hydraulics Laboratory (HL), under the direction of Messrs. Frank A. Herrmann, Jr., Chief of the HL; Glenn A. Pickering, Chief of the Hydraulic Structures Division (HSD); and John L. Grace, Jr., former Chief of the HSD. The effort was supported by the Water Quality Research Program (WQRP), Work Unit 32366, entitled "Evaluation of Blending Characteristics of Single Wet Well Structures." The WQRP is sponsored by the Headquarters, US Army Corps of Engineers (HQUSACE), and is assigned to the Environmental Laboratory (EL), WES. The HQUSACE Technical Monitor is Mr. David P. Buelow. Mr. J. Lewis Decell, EL, is the WES Program Manager of the WQRP; Dr. Jerome L. Mahloch was the former Program Manager of the WQRP. Dr. John Harrison is Chief, EL.

This study was conducted under the direct supervision of Dr. Jeffery P. Holland, Chief of the Reservoir Water Quality Branch (RWQB), and Dr. Richard E. Price, former Chief of the RWQB. Mr. Stacy E. Howington prepared this report. Assisting in the testing were Messrs. Jack E. Davis; Calvin Buie, Jr.; Douglas M. White; and Paul Ahlrich; and Ms. Karen R. Ingram. Data were provided by Messrs. Charles H. Tate, Jr., and Mark S. Dortch and the US Army Engineer Districts, Portland (NPP), Sacramento, and Louisville. Mr. Richard A. Cassidy, NPP, provided technical assistance in the form of multiple data sets and other information. Dr. Holland and Mr. Steven C. Wilhelms contributed significantly in the initial development of the theory. The report was edited by Ms. Lee T. Byrne of the Information Technology Laboratory.

Commander and Director of WES during publication of this report was COL Larry B. Fulton, EN. Dr. Robert W. Whalin was Technical Director.

This report should be cited as follows:

Howington, Stacy, E. 1990. "Simultaneous, Multiple-Level Withdrawal from a Density Stratified Reservoir," Technical Report W-90-1, US Army Engineer Waterways Experiment Station, Vicksburg, MS.

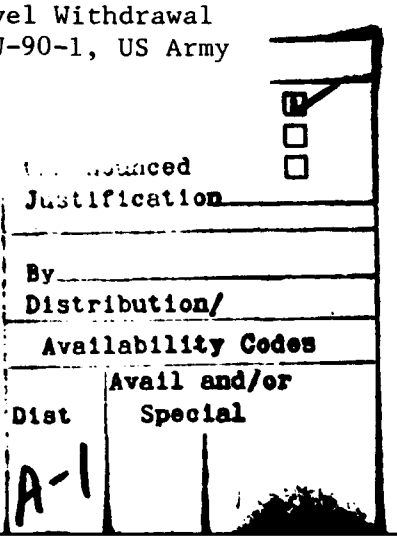

CONTENTS

SIMULTANEOUS, MULTIPLE-LEVEL WITHDRAWAL FROM A DENSITY STRATIFIED RESERVOIR

PART I: INTRODUCTION

General

1. An integral part of effectively operating a hydraulic structure by the US Army Corps of Engineers (CE) is environmentally sound use of the natural resources. In this light, it is of great importance that the man-made reservoirs across the Nation be operated in a manner that is not only nondegrading, but is also beneficial to the in-reservoir and downstream ecosystems.

2. Many reservoirs develop significant temperature differences among horizontally oriented strata during the warmer months of the year. This is primarily due to generally higher heat influx and lower flow rate through the reservoir during this period and to the physical relationship between water temperature and water density. Much of the thermal energy entering a reservoir is absorbed in the upper layers, making them lighter, while the lower layers remain cooler and denser. Vertical transport and exchange among the horizontal strata are inhibited by buoyancy. As a result, vertical stratification of other constituents such as dissolved oxygen and dissolved metals is also common, and different strata may be vastly different in composition.

3. Selective withdrawal is the withdrawal of water from a specified vertical range in a stratified reservoir. It is possible because of the limited vertical movement of fluid imposed by density stratification, and it permits control of the quality of water released. Operation of a single intake port is sometimes adequate to meet a release water quality objective. However, it is often necessary to withdraw from multiple intake ports at different elevations and to mix the different water qualities withdrawn from each elevation to achieve a desired result.

4. Dual-wet-well, dual-flow-control reservoir intake structures have served this purpose in the past. In the conventional operation of these structures, one intake port in each wet well may be opened. The amount of flow that passes through each of the intake ports is easily managed by service gates at the exit of each wet well. Mixing of the different water qualities occurs downstream of the service gates.

5. Operating in a dual-wet-well, dual-flow-control mode is not always possible. For example, in recent years, the addition of hydropower to existing dams has become an attractive source of renewable energy. This often involves the addition of hydroturbines to the downstream end of the existing release conduit, which normally requires the relocation of flow control from the service gates to the hydroturbines. If the hydroturbines use a common penstock, as is normally the case in a retrofit, the distribution of flow through multiple open intakes is no longer strictly controlled. Operation of multiple intake ports with a common, downstream flow control allows density stratification in the reservoir to influence the flow distribution among the open ports.

6. At sites with hydropower, dual-wet-well structures may not provide an advantage in operational flexibility over single wet wells unless dual-flow controls can be maintained. For this reason and for potential cost savings offered by construction of a single well, single-wet-well structures are becoming increasingly popular for selective withdrawal structure additions and for new dam construction.

Objectives

7. The objectives of this work are to demonstrate that in a density-stratified environment:

a. Multiple intake ports upstream of a single-flow control can be employed simultaneously in the interest of water quality.

b. The flow distribution among the open ports can be satisfactorily approximated using algebraic techniques.

This approach is chosen because numerical solution of the three-dimensional (3-D) Navier-Stokes equations for the flow phenomenon under investigation is difficult and expensive and because simplicity and portability are necessary to ensure widespread use of the technology in locations where large-scale computing facilities are not available.

Scope

8. A series of approximate expressions based on the Euler equation for increasingly complex situations is developed to compute the stratification-influenced port flow rates. Work concentrates on the simplest case: the

multiported, single-wet-well intake structure. The assumptions employed in this development and the limitations of the applicability of the expression are given in detail. The resulting algorithm for predicting flow rates is compared with previously collected prototype and physical model data. The information gained provides for the creation of a predictive tool for effective single-flow-control structure operations and produces some guidance for the design of future structures or structure modifications.

9. The results of this effort permit prediction, and partial control of, the flow distribution among intake ports in a stratified environment without individual flow-control devices. Existing selective withdrawal technology is coupled with this capability in reservoir intake structure operation to predict and/or control release water quality.

10. The implications of this improvement in operational capabilities reach further than the hydropower addition and single-wet-well applications previously discussed. Benefits might also extend to existing dual-wet-well, dual-flow-control structures with the need for increased operational flexibility. Each of the wet wells could be operated as multiported, single-wet-well structures to achieve more closely the desired objectives. Other situations such as emergency or maintenance shutdown of one wet well in a dual-well structure might no longer entail a sacrifice in release water quality control if the remaining well could be operated with multiple intake ports. Additionally, existing single-flow-control, multiported structures would no longer be limited to confident operation of one port at a time. In short, multilevel withdrawal might facilitate the achievement of water quality and energy development interests at the same reservoir.

PART II: REVIEW OF LITERATURE

11. A literature review of simultaneous, multiple-level withdrawal from a density-stratified reservoir involves several general areas:

a. Reservoir stratification.

b. Selective withdrawal.

c. Simultaneous, multiple-level withdrawal.

d. Head-loss descriptions in hydraulic structures.

Reservoir Stratification

12. During the warmer months, it is not uncommon for reservoirs to develop significant thermal and density stratification patterns in the vertical, as discussed by Hutchinson (1957), Kittrell (1965), and Wetzel (1975). The physical relationship between temperature and density for water (Figure 1) makes stratification possible. For pure water above 4° C, temperature is inversely proportional to density. The surface waters of a reservoir absorb heat through solar radiation and atmospheric exchange. Heating of these waters increases their buoyancy. Conversely, the deeper waters receive less thermal influx and remain cooler and denser.

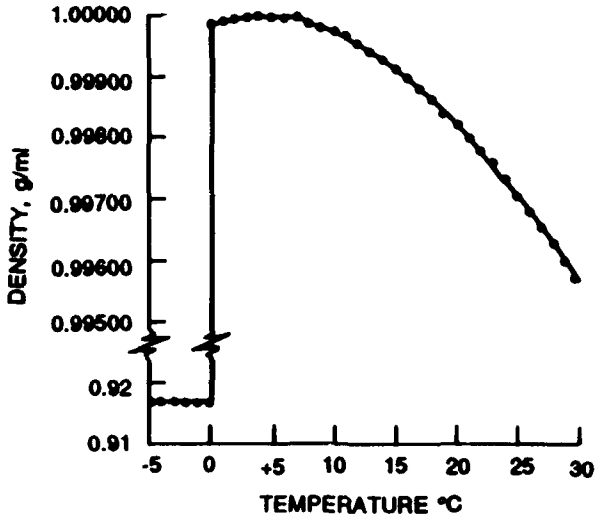

Figure 1. Density as a function of temperature (modified from Wetzel (1975))

13. Density stratification of this sort is self-maintaining in that buoyancy limits the mixing among temperature strata. Some convective mixing in the upper layers of the pool is common due to wind effects and to diurnal fluctuations in the surface temperature. The result is often a reservoir like that in Figure 2 that has three distinct layers: a mixed lower layer called the hypolimnion, a mixed upper layer called the epilimnion, and a transition layer called the metalimnion. The metalimnion contains the sharpest temperature and density gradients, referred to as the thermocline and pycnocline, respectively.

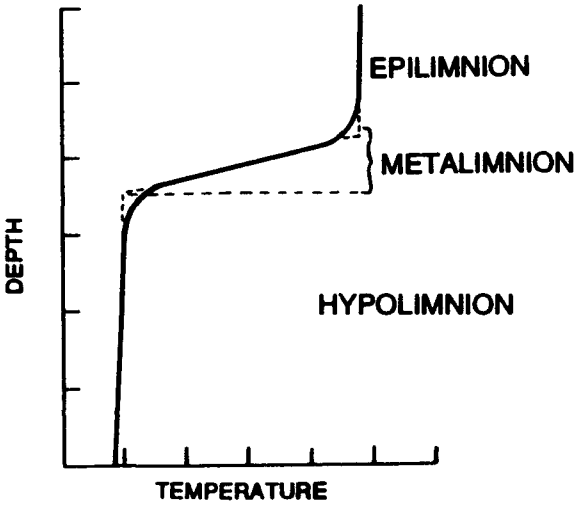

Figure 2. Typical reservoir thermal stratification (modified from Wetzel (1975))

14. Stratification of temperature and density often leads to stratification of other water quality components. As stated by Wetzel (1975), "Without question, the regulation of the entire physical and chemical dynamics of lakes and the resultant metabolism is governed to a very great extent by differences in density." Stratification plays an important role in the management of in-reservoir and release water quality.

15. Lagler (1956) describes the in-reservoir movement of fish as a result of the temperature stratification. Cramer et al. (1985) discuss the significant impact of temperature and flow on the behavior and survival rate of salmonids downstream of operating reservoirs in the Northwest. These and other studies suggest that proper fisheries management often requires that

in-reservoir and downstream water qualities be predictable and partially controllable.

Selective Withdrawal

16. Reservoir stratification and reservoir withdrawal are interdependent processes. The elevation of the withdrawal device and the withdrawal quantity partially dictate the reservoir composition by the selective removal of reservoir resources. In-reservoir withdrawal patterns are, in turn, dependent on the reservoir stratification.

17. Selective withdrawal is a common technique that makes use of the interdependence between stratification and withdrawal to control in-reservoir and release water quality. The limited vertical flow imposed by the density stratification often permits a sink such as an open intake port to withdraw water from a confined vertical range. Selective withdrawal has been widely studied both analytically and experimentally. However, much of the work to date has been confined to two-layer or linear density stratification, examples of which are given in Figure 3.

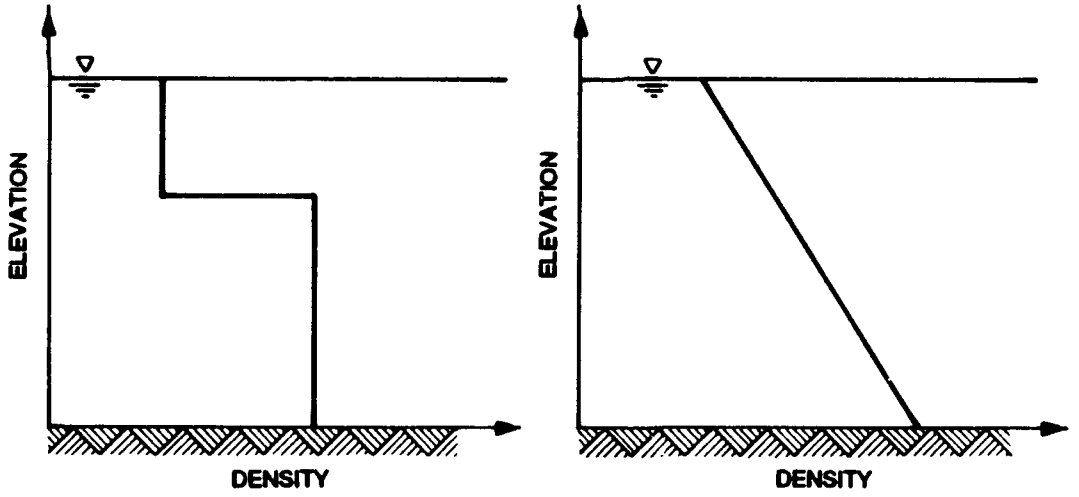

a. Two-layer stratification b. Linear stratification

Figure 3. Example two-layer and linear density stratification patterns

18. A thorough review of selective withdrawal research and the interrelations among the approaches has been provided by Smith et al. (1987). Craya (1949) analytically examined two-layer stratification with a single

point sink located in a vertical face. Although a port is not actually a point sink (a sink with infinitesimally small physical dimensions), the point-sink approximation is satisfactory when an intake is very small compared with the thickness of the region from which withdrawal occurred (the withdrawal zone). Craya sought to establish the critical densimetric Froude number at which withdrawal from both layers occurred. Gariel (1949) verified the analytic results of Craya through laboratory experiments.

19. Further analytic and experimental work in two-layer stratification by Harleman, Morgan, and Purple (1959) investigated the critical densimetric Froude number for incipient flow from the upper layer into a sink located in the floor of the test flume. Lawrence and Imberger (1979) experimentally evaluated incipient withdrawal from the lower of two layers into a surface sink.

20. Research with linear stratification patterns has focused predominantly on the limits of withdrawal rather than on a critical densimetric Froude number. Limits of withdrawal define the withdrawal zone far from the sink, where the streamlines are virtually horizontal. Several researchers such as Hino and Furusawa (1969), Croach (1971), Hino (1980), and Farrant (1982) have studied withdrawal limits for linear stratification.

21. Studies of withdrawal from arbitrarily stratified fluids have been less abundant than those for two-layer or linear stratification. Arbitrary stratification is important in the practical application of selective withdrawal since reservoir stratification patterns may not resemble either two-layer or linear stratification.

22. Bohan and Grace (1969, 1973) experimentally studied selective withdrawal from an arbitrarily stratified fluid through a point sink in a vertical face. Their research produced the following equation to describe the limits of withdrawal away from vertical boundaries.

$$V_o = \frac{Z^2}{A_o}\sqrt{\frac{\Delta\rho g Z}{\rho}} \tag{1}$$

where

V_o = average velocity through the orifice, m/sec

Z = vertical distance between the orifice center line and the limit of withdrawal, m

A_o = area of the orifice, m^2

$\Delta\rho$ = density difference between the orifice center line and the limit of withdrawal, kg/m^3

g = gravitational acceleration, m/sec^2

ρ = density at the orifice center line, kg/m^3

When boundary interference was encountered (that is, when the limit of withdrawal intersected the water surface or the flume bottom), the interfering boundary was taken as the limit of withdrawal, and Equation 1 was not applicable for that limit.

23. Since a description of the withdrawal requires not only that the limits of withdrawal be established, but also that the flow distribution within the withdrawal zone be determined, Bohan and Grace (1973) developed Equation 2, which relates the density distribution to the normalized vertical velocity profile resulting from withdrawal, as follows:

$$\nu = \frac{v}{V} = \left(1 - \frac{y}{Y}\,\frac{\Delta\rho}{\Delta\rho_m}\right)^2 \qquad (2)$$

where

ν = normalized velocity for the vertical point of interest

v = local velocity at the point of interest, m/sec

V = maximum velocity in the profile, m/sec

y = distance between the center line of the orifice and the point of interest, m

Y = distance between the center line of the orifice and the limit of withdrawal, m

$\Delta\rho$ = density difference between the center line of the orifice and the point of interest, kg/m^3

$\Delta\rho_m$ = density difference between the orifice center line and the limit of withdrawal, kg/m^3

This velocity profile applies to the withdrawal zone at some horizontal distance from the orifice where the flow is essentially unidirectional. Integration of Equation 2 over the withdrawal zone thickness produces a withdrawal profile that permits the direct computation of the release water quality from the in-reservoir profiles.

24. Smith et al. (1987) generalized Equation 1 by defining the withdrawal angle. This angle, measured in the horizontal plane with the vertex at

the point sink, includes the geometry of the near field in the selective withdrawal description (Figure 4). For example, Equation 1 was developed for a point sink in a vertical face that produces a withdrawal angle of pi radians.

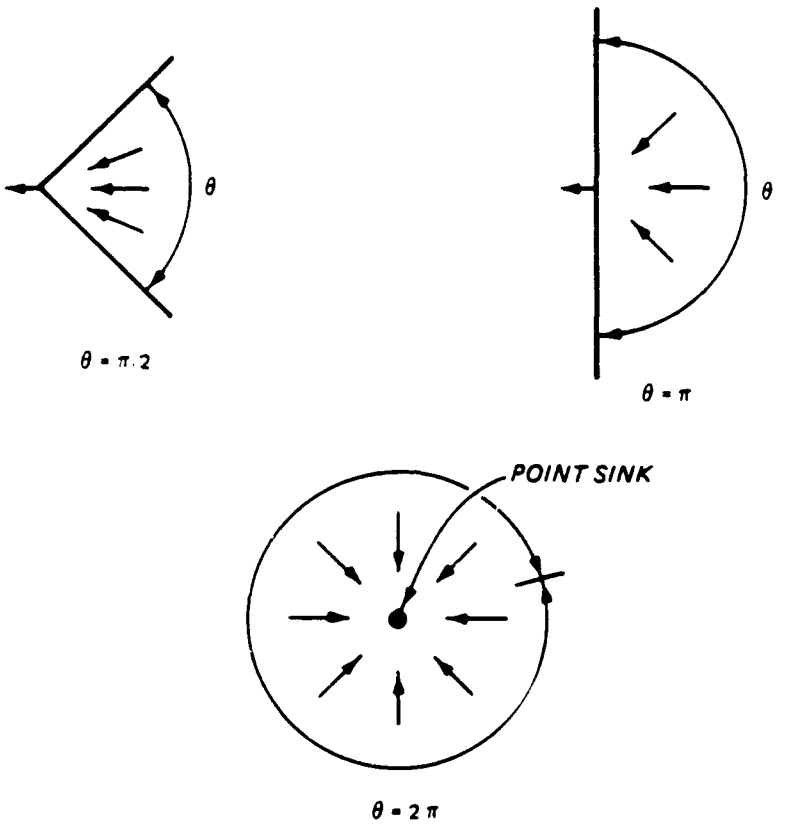

Figure 4. Schematic plan of various withdrawal angles, after Smith et al. (1987)

25. Smith et al. (1987) developed Equation 3 for description of the in-pool limit of withdrawal when the other limit experienced interference from a boundary. Equation 1, with a modification to include the withdrawal angle, has been combined with Equations 2 and 3 in the SELECT one-dimensional (1-D) mathematical model described by Davis et al. (1987) to produce a reservoir withdrawal model capable of predicting release water composition and in-reservoir withdrawal patterns for arbitrary stratifications.

$$\frac{Q}{D^3 N} = \frac{\theta}{2\pi} \frac{\left[1 + \frac{1}{\pi} \sin\left(\frac{b/D}{1 - b/D}\,\pi\right) + \frac{b/D}{1 - b/D}\right]}{\left(\frac{b/D}{1 - b/D}\right)^3} \qquad (3)$$

where

Q = flow through the point sink, m^3/sec

D = distance between the boundary of interference and the free limit of withdrawal, m

N = buoyancy frequency, sec^{-1}

θ = effective angle of withdrawal, radians

π = mathematical constant (3.14159), radians

b = distance between the point sink and the boundary of interference, m

Simultaneous, Multiple-Level Withdrawal

26. Simultaneous multiple-level withdrawal from stratified reservoirs has been addressed by Bohan and Gloriod (1972) and Bohan and Grace (1973). These studies focused on the interaction between overlapping withdrawal zones in the pool. In each case, the distribution of the total flow between the open ports was strictly controlled by individual flow-control devices. Bohan and Grace (1973) proposed that density stratification might block flow from the upper of two ports in a single wet well.

27. Little work has been done regarding the blocking problem identified by Bohan and Grace (1973) because the need for simultaneous, multiple-level withdrawal has been largely unrecognized.

28. Tate and Dortch* performed the initial experiments with simultaneous, multiple-level withdrawal, concentrating on the flow through two ports in a single-wet-well physical model with two-layer stratification. Several points can be made regarding their raw data and data analysis procedures.

29. The researchers employed extensive use of fluorometry. One layer of the two-layer stratification was dyed with fluorescent dye, and the release water was passed through a fluorometer to determine its dye concentration. From the known dye concentrations in the two layers and from the assumption that the flow entering each port contained only water from one layer, the flow distribution was computed by mass balance. They then developed an empirical formula for the fraction of total discharge through the upper port:

---

* C. H. Tate, Jr., and M. S. Dortch, 1983, unpublished data, US Army Engineer Waterways Experiment Station, Vicksburg, MS.

$$\frac{Q_u}{Q} = 0.5 - 0.5e^{[-0.85(X-1)]} \quad (4)$$

with

$$X = \frac{Q}{CA\sqrt{\frac{2g\Delta\rho H_A}{\rho}}}$$

where

Q_u = upper port flow, m^3/sec

Q = total discharge, m^3/sec

e = natural logarithm base (2.7128)

C = discharge coefficient for orifice

A = area of orifice, m^2

$\Delta\rho$ = density difference between the two layers, kg/m^3

H_A = actual pycnocline displacement in the wet well when flow from the upper port was observed, m

ρ = density of the lower layer, kg/m^3

30. Tate and Dortch (unpublished data) also proposed analytically that the discharge must overcome an additional head loss imposed by the buoyancy. If the flow was insufficient to overcome this buoyancy head, thermal blockage was said to exist. The term "thermal" referred to the temperature difference between the layers, but the corresponding density difference was the source of the blockage. This buoyancy head was described by

$$h1 = \frac{\Delta\rho}{\rho} d_2 \quad (5)$$

where

$h1$ = head loss due to buoyancy head, m

d_2 = distance between the pycnocline and the lower port center line, m

31. Since the wet well was large compared with the port dimensions, Tate and Dortch neglected skin friction losses between the ports in their

proposal. They apparently, however, never compared the experimental data with the analytic expressions.

32. Howington (1986, 1987, 1988) has addressed the computation of flow distribution among multiple ports in single-wet-well structures. The present work expands and completes that of earlier investigations.

Head-Loss Description

33. The calculation of head loss as water passes through or around hydraulic structures is still an empirical science, and many publications have been devoted to this subject. Once of the simplest and most widely used equations is a form of the Darcy-Weisbach equation given in hydraulics texts such as Brater and King (1976), Vennard and Street (1975), Streeter and Wylie (1975), and US Army, Office, Chief of Engineers (1968). It employs a single coefficient to replace the f(L/D) term in the original Darcy-Weisbach equation; i.e.,

$$hl_f = k\frac{V^2}{2g} \tag{6}$$

where

hl_f = head loss due to friction, m of water

k = head-loss coefficient

V = velocity, m/sec

Miller (1978) discusses the computation of head-loss coefficients for inlet manifolds and the subsequent, iterative computation of flow distribution among the intakes of the manifold for uniform density. This is analogous to the computation of flow distribution among multiple ports for a single-flow-control intake structure in a reservoir without stratification.

34. In summary, the process of reservoir stratification and its importance in reservoir ecology is recognized. Selective withdrawal has been extensively researched and is being successfully used as a tool in reservoir and reservoir-release water quality management. Only the in-reservoir aspects of simultaneous, multiple-level withdrawal from a stratified reservoir have been studied. These studies have examined the effects of overlapping

withdrawal zones, assuming that the individual port flows were known, which at present requires individual flow control for each port.

35. Preliminary investigations into the effects of density stratification on flow distribution among multiple open ports have been performed, but no generalizations have been made. Effective use of selective withdrawal requires that these density influences be resolvable.

PART III: ALGORITHM DEVELOPMENT

36. An algorithm was needed that predicted the flow distribution among multiple, open ports in a single-flow-control intake structure and that could be used by project personnel for real-time operational decisions. Accurate numerical modeling of the 3-D hydrodynamics was impractical for real-time operations decision-making, so an approximation was sought for the steady state. For the desired purpose, the solution need not produce a description of the velocity field, the boundary layer effects, or the like, within the well.

37. A form of the Euler equation, derived in the Appendix A, was chosen to describe the flow distribution approximately. The assumptions made by selecting this equation are outlined below. The development of the algorithm for the general reservoir was similar to that for selective withdrawal in the literature review. That is, work began with the simplest possible case (two-layer stratification) and proceeded toward the more difficult and more practical applications.

Two-Layer Stratification

38. Consider the idealized situation in Figure 5. This represents a reservoir intake structure with two intake ports. There are two density strata with an infinitesimally thin interface between the lighter, upper layer and the heavier, lower layer. One port is located well within each respective

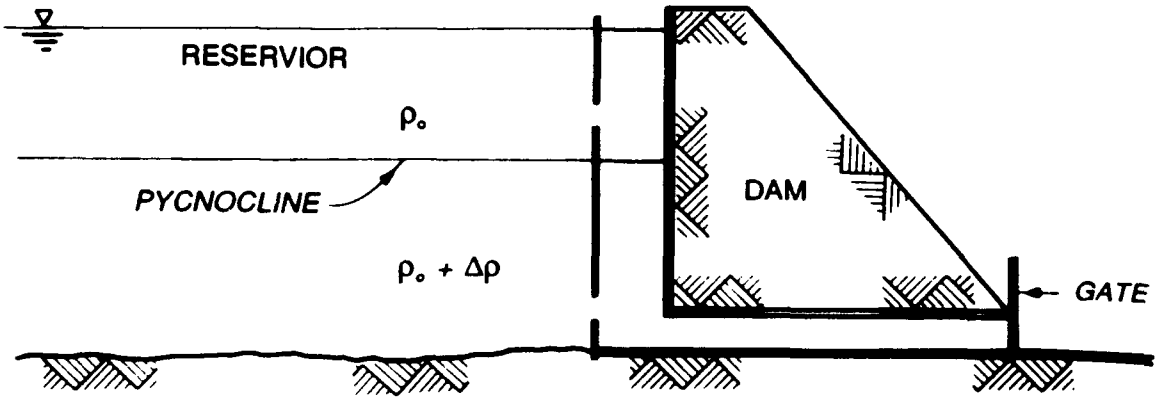

Figure 5. Two-port intake structure in a two-layer stratification with no flow

layer, and each port is assumed to withdraw water only from the layer in which it is located. The only flow control is the service gate at the exit from the structure, and the intake ports are identical in size, shape, and loss coefficient.

39. Initially, the system is at rest as depicted in Figure 5. Buoyancy considerations dictate that the density stratification in the wet well (the vertical passage inside the structure) closely resemble that of the pool. They need not be identical, but they must produce the same hydrostatic pressure across each of the open ports.

40. With a very small, steady discharge from the structure (Figure 6a), all flow is withdrawn through the lower port. Therefore, the release density equals the density of the lower layer. No water-surface drop occurs in the wet well since no flow passes through the upper port in the steady state. The upper port flow is blocked by the density stratification (a condition referred to as buoyancy blockage). A drop in the elevation of the pycnocline occurs in the wet well because of the loss of energy from the flow entering the lower port. A slightly higher discharge would result in a lower pycnocline in the well.

41. The trend of lowered pycnocline elevation with increased discharge cannot continue indefinitely. Theoretically, once the pycnocline elevation reaches that of the lower port (Figure 6b), a critical equilibrium will be achieved. Any increase above this theoretical critical discharge would induce flow from the upper port, and the release water would be composed of water from both layers. Flow through the upper port will be accompanied by a drop in the water surface elevation in the well.

42. A quantitative description of the steady flow distribution for a two-layer stratification was obtained from the Euler equation. First, a means of determining critical discharge was developed. The Euler equation was applied along the streamline passing through points 2 and 3 and across the lower intake, as shown in Figure 6b:

$$\frac{V_2^2}{2} + gz_2 = \int_2^3 \frac{dp}{\rho} + \frac{V_3^2}{2} + gz_3 + losses_{2-3} \qquad (7)$$

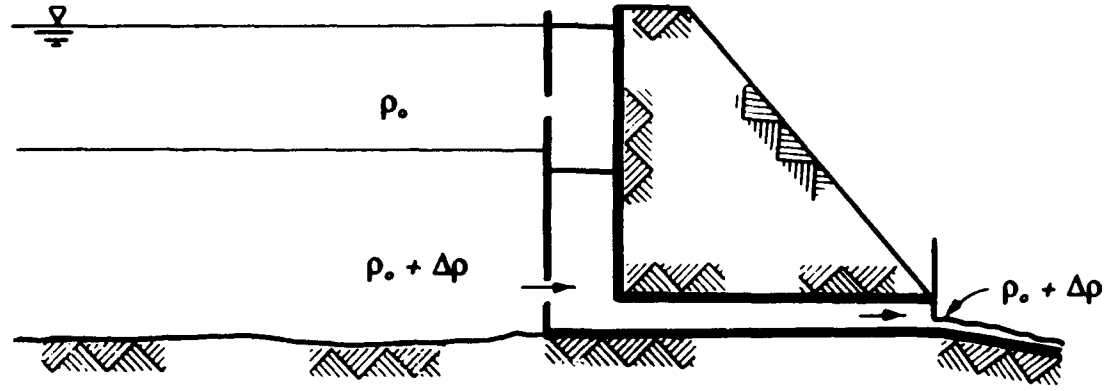

a. Small discharge

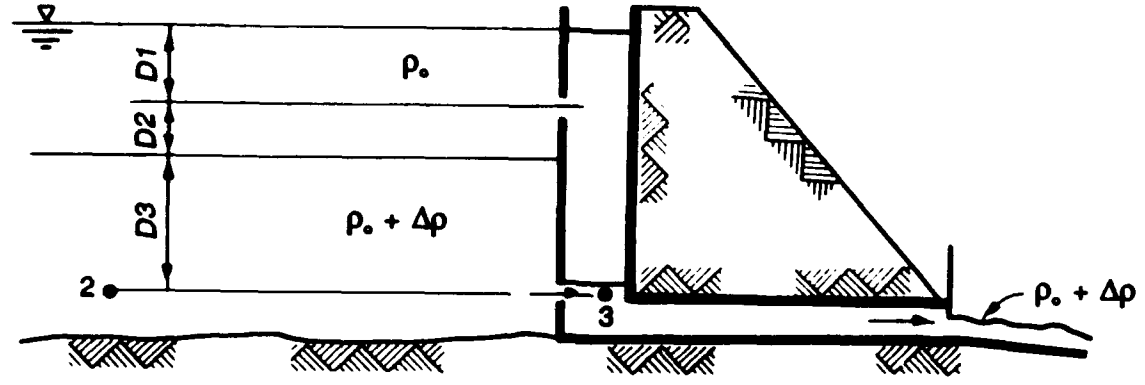

b. Theoretical critical discharge

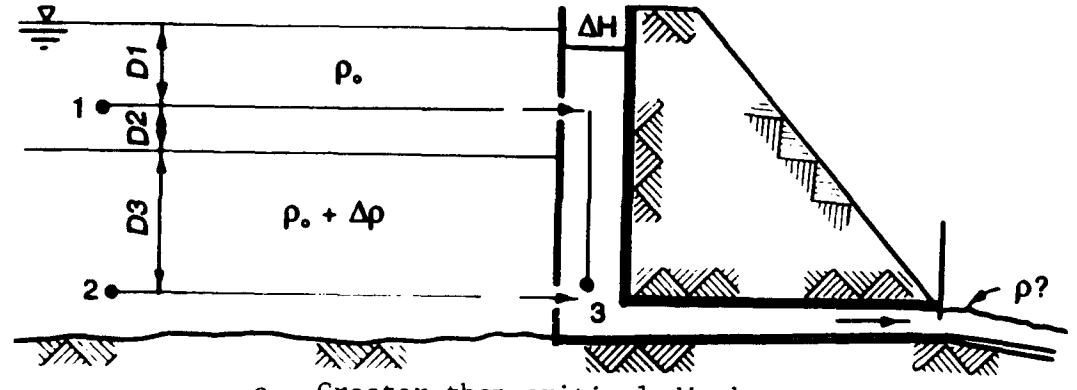

c. Greater than critical discharge

Figure 6. Response of ideal structure to increasing discharges

where

V_2, V_3 = velocity at points 2 and 3, respectively, m/sec

g = gravitational acceleration, m/sec^2

z_2, z_3 = height of points 2 and 3, respectively, above a datum, m

p = pressure, N/m^2

ρ = mass density, kg/m^3

$losses_{2-3}$ = energy losses per unit mass between points 2 and 3, m^2/sec^2

43. The velocity of the fluid at point 2 in the reservoir is assumed small, so its contribution to the total energy at point 2 is negligible. Points 2 and 3 are also located on the same horizontal plane, so $z_2 = z_3$. Dividing through by g converts the remaining terms into equivalent depth of water and leaves

$$\varnothing = \int_2^3 \frac{dp}{g\rho} + \frac{V_3^2}{2g} + hl_{2-3} \tag{8}$$

where hl_{2-3} = head loss (in depth of water), m. Assuming that the pressures at points 2 and 3 are hydrostatic, assuming the kinetic energy at point 3 is consumed by turbulent eddy development in the well, and evaluating the pressure integral, yields

$$D3\left(\frac{\Delta\rho}{\rho_o + \Delta\rho}\right) = hl_{2-3} \tag{9}$$

where

$D3$ = height of the pycnocline in the reservoir above the lower port, m

Δp = density difference between the layers, kg/m^3

ρ_o = density of the upper layer, kg/m^3

44. By describing this head loss as a function of the port velocity squared (Equation 6), the critical discharge can be computed as follows:

$$QC = \sqrt{\frac{2gA_1^2 D3\Delta\rho}{k(\rho_o + \Delta\rho)}} \tag{10}$$

where

QC = critical discharge, m^3/sec

A_1 = area of the lower port, m^2

k = head-loss coefficient for lower port

45. Equation 10 produces a conservative approximation for the total discharge needed to induce flow through the upper port, because the lower port velocity jet that impinges on the back wall of the wet well does not permit the pycnocline to be drawn down intact to the top of the lower port. This phenomenon will be addressed later.

46. To describe the distribution of flow among multiple open ports like those in Figure 6c, a procedure similar to that for the critical discharge is followed. The Euler equation can be written simultaneously between points 2 and 3 across the lower port and between points 1 and 3 across the upper port. Point 3 is assumed to be the point at which mixing of the water from the two ports occurs. By the definition of a streamline, no flow can cross the path from 1 to 3 or the one from 2 to 3. Therefore, it is assumed that point 3 is located exactly at the juncture of the two streamlines. Neglecting the in-pool velocities like in the critical discharge determination and dividing through by g , one obtains the following equations:

$$z_1 = \int_1^3 \frac{dp}{g\rho} + \frac{V_3^2}{2g} + z_3 + h1_{1-3} \tag{11}$$

$$\varnothing = \int_2^3 \frac{dp}{g\rho} + \frac{V_3^2}{2g} + h1_{2-3} \tag{12}$$

47. Miller (1978) suggests that the frictional losses between the intakes in a manifold may be neglected. Making this assumption for intake structures and using the hydrostatic approximation for the pressure at point 3 then gives

$$D2 + D3 + \frac{D1\rho_o}{\rho_o} - \frac{(D1 + D2 + D3 - \Delta H)\rho_o}{\rho_o} - \frac{V_3^2}{2g} = h1_{1-3} \quad (13)$$

$$\frac{(D1 + D2)\ \rho_o + D3\ (\rho_o + \Delta\rho)}{(\rho_o + \Delta\rho)} - \frac{(D1 + D2 + D3 - \Delta H)\ \rho_o}{(\rho_o + \Delta\rho)} - \frac{V_3^2}{2g} = h1_{2-3} \quad (14)$$

where

$D2$ = elevation difference between the upper port center line and the pycnocline, m

$D3$ = elevation difference between the pycnocline and the lower port center line, m

$D1$ = elevation difference between the water surface and the upper port center line, m

ΔH = water surface differential between the pool and the well, m

Canceling terms in Equations 13 and 14 and neglecting the kinetic energy at point 3, as in Equation 9, produces

$$h1_{1-3} = \Delta H \quad (15)$$

$$h1_{2-3} = \frac{\Delta\rho D3 - \Delta\rho\Delta H}{\rho_o + \Delta\rho} \quad (16)$$

In practice, $\Delta p \Delta H$ can also be neglected since ΔH will be small compared with $D3$. Substitution of Equation 15 into Equation 16 results in the following relationship between the head losses:

$$h1_{2-3} = h1_{1-3} + \frac{\Delta\rho D3}{\rho_o + \Delta\rho} \quad (17)$$

The difference between the two head losses is due strictly to the density stratification and is called the buoyancy head. The shaded area in Figure 7 represents the numerator in the buoyancy head.

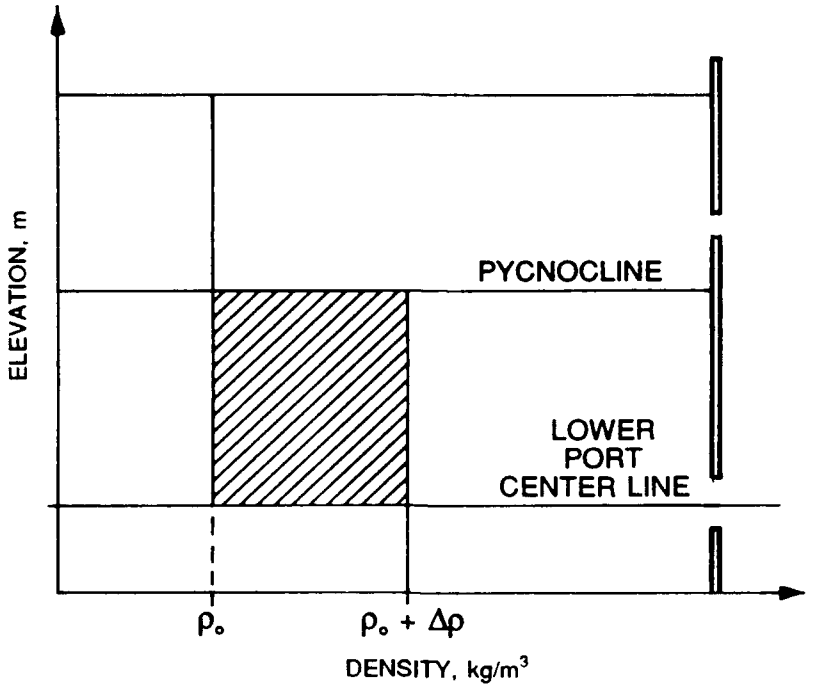

Figure 7. Numerator of the buoyancy head for two-layer stratification

48. To convert the relationship between the head losses to one of discharges, again Equation 6 was applied. Since the total discharge will equal the sum of the two port flows (Equation 18), there follows the relationship (Equation 19) in which the only remaining unknown, assuming the loss coefficients can be approximated, is the water surface drop in the wet well.

$$QT = QU + QL \tag{18}$$

$$QT = \sqrt{\frac{2gA_u^2}{k_u}\,\Delta H} + \sqrt{\frac{2gA_1^2}{k_1}\left(\Delta H + \frac{\Delta\rho D3}{\rho_o + \Delta\rho}\right)} \tag{19}$$

where

QT = total structure discharge, m^3/sec

QU = upper port flow, m^3/sec

QL = lower port flow, m^3/sec

A_u = area of the upper port, m^2

k_u = loss coefficient for the upper port

49. An iterative solution to this equation is simple. Either a flow distribution can be assumed, the ΔH computed, the total discharge computed, and the flow distribution modified; or a ΔH can be estimated, the total discharge computed, and ΔH modified until agreement is reached. Figure 8 demonstrates the relationship between total discharge and upper port flow for Equation 19 for an assumed set of loss coefficients, buoyancy head, and $D3$ values.

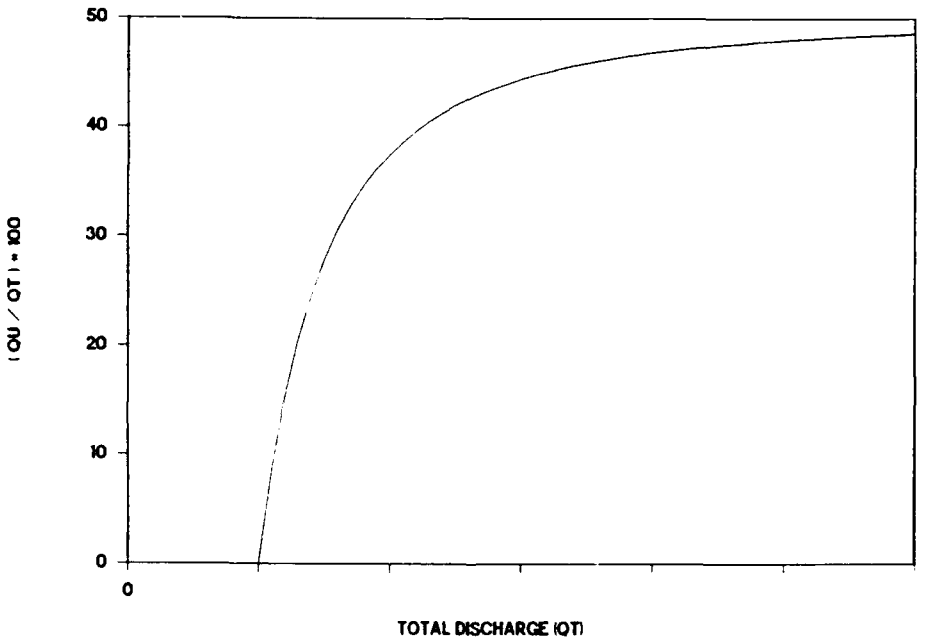

Figure 8. Percentage of total discharge through the upper port versus total discharge for a single stratification

50. Buoyancy blockage is evident in Figure 8 at very low total discharges for which the upper port flow percentage is zero. The discontinuity in the curve represents the theoretical critical discharge. At this discharge, flow from the upper port is incipient. The effects of density on the flow distribution diminish as the total discharge increases. The buoyancy-head term in Equation 19 remains constant as the discharge increases, while the head losses increase proportional to the port flows squared. This explains the diminishing effect of density stratification at high flows. The effects of density would be nonexistent when the curve reached the 50-percent

mark for flow through the upper port for these identically defined ports. This is the flow distribution expected in a uniform density pool, neglecting skin-friction losses in the well.

Linear Stratification

51. When the density stratification pattern is linear, only a few modifications to the preceding description are needed. Further attention must be given to the density of the water entering the ports. However, for linear stratification and intermediate withdrawal conditions, the density entering the port will be approximately equal to the density in the pool at the elevation of the port (Smith et al. 1987). Intermediate withdrawal requires that the limits of withdrawal be freely established (no boundary interference).

52. For theoretical critical discharge, the head loss through the lower port must overcome the buoyancy head between the port levels. Assuming intermediate withdrawal and linear stratification, the critical discharge is

$$QC = \sqrt{\frac{2gA_1^2 D2(\rho_2 - \rho_1)}{2k_1\rho_2}} \tag{20}$$

where

$D2$ = elevation difference between port center lines, m

ρ_2 = density at the center line of the lower port, kg/m^3

ρ_1 = density at the center line of the upper port, kg/m^3

53. For flows larger than theoretical critical discharge, the description follows the two layer work closely. Assuming that the stratification above the highest port in the wet well is the same as that in the pool, the linear-stratification equivalent of Equation 17 is

$$h1_{2\text{-}3} = h1_{1\text{-}3} + \frac{D2(\rho_2 - \rho_1)}{2\rho_2} \tag{21}$$

The buoyancy head for the linear-stratification condition is the shaded area in Figure 9 divided by the density at the center line of the lower port. The

relationship between the flows for both ports is derived as it was for Equations 18 and 19 in the two-layer work and is given in Equation 22.

$$QT = \sqrt{\frac{2gA_u^2}{k_u}\Delta H} + \sqrt{\frac{2gA_1^2}{k_1}\left(\Delta H + \frac{\rho_2 - \rho_1}{2\rho_2} D2\right)} \tag{22}$$

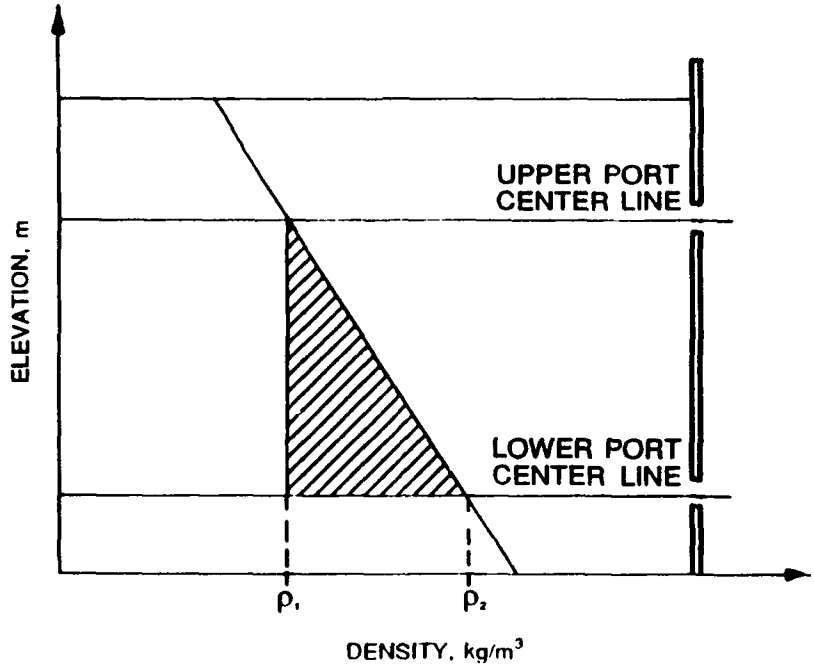

Figure 9. Numerator of the buoyancy head for linear stratification

Arbitrary Stratification

54. As was pointed out by Bohan and Grace (1973), reservoir density stratification resulting primarily from temperature is seldom two-layer or linear. Practical application to reservoirs requires that the description of flow distribution among the ports be extended to arbitrary stratification.

55. Theoretical critical discharge can be described for arbitrary stratification much as it was for two-layer and linear stratifications, with the only difference being the need to compute the density entering the lower port. During the establishment of steady state, a very small flow will enter the upper port to fill the void created by the pycnocline drawdown in the wet well. The density of this flow is very close to the center-line density of

the upper port. However, the larger flow entering the lower port may have a density measurably different from the lower port center-line density. Thus, the Euler equation must be written along the streamline containing the density withdrawn through the lower port as seen in Figure 10. This logic assumes that the fluid entering the port is fully mixed and this mixing does not violate the streamline declaration.

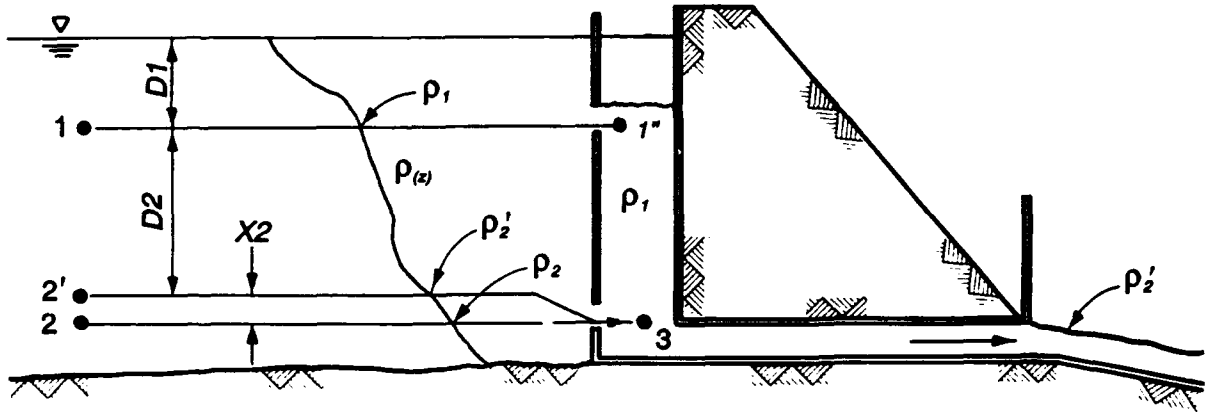

Figure 10. Definition sketch for critical discharge with an arbitrary stratification

56. The water in the wet well between the port elevations is replaced with water that has the center-line density of the upper port. Point 2 is located at the elevation of the lower port center line, and point 2′ coincides with the density withdrawn through the lower intake. After applying the Euler equation between points 2′ and 3 and simplifying as in the previous derivations, the following equation results:

$$h1_{2'-3} = \frac{1}{g\rho_{2'}} \int_{ws}^{2'} g\rho(z)\,dz - \frac{1}{g\rho_{2'}} \int_{ws}^{3} g\rho_1 dz + X2 \qquad (23)$$

where

$\rho_{2'}$ = density entering the lower port, kg/m^3

ws = elevation of the water surface in the reservoir, m

$\rho(z)$ = density as a function of depth, kg/m^3

z = depth measured down from the water surface, m

ρ_1 = density of the water at the center line of the upper port, kg/m^3

$X2$ = elevation difference between the lower port center line and the streamline containing the density entering that port, m

57. The first term on the right side of Equation 23 represents the pressure head at point 2', and the second term, the pressure head in the well at point 3. If the pressure integrals are broken into parts, Equation 23 becomes simpler. As before, it is assumed that the stratification in the wet well is the same as that in the pool above the upper port. Point 1 is located in the pool at the elevation of the upper port, and 1" is located in the well at the same elevation. This leaves

$$h1_{2'-3} = \frac{1}{g\rho_{2'}} \int_1^{2'} g\rho(z)\,dz - \frac{1}{g\rho_{2'}} \int_{1''}^{3} g\rho_1 dz + X2 \tag{24}$$

Noting that

$$X2 = \frac{1}{g\rho_{2'}} \int_{2'}^{2} g\rho(z)\,dz \tag{25}$$

Equation 24 is further reduced to

$$h1_{2'-3} = \frac{1}{\rho_{2'}} \int_1^2 [\rho(z) - \rho_1]\,dz \tag{26}$$

Equation 26, which describes the head loss associated with the theoretical critical discharge, can be easily converted to a flow rate as was done in Equations 10 and 20. This produces the following equation for theoretical critical discharge, which applies in any stable stratification pattern for two levels of withdrawal:

$$QC = \sqrt{\frac{2gA_1^2}{k_1\rho_{2'}} \int_1^2 [\rho(z) - \rho_1]\,dz} \tag{27}$$

58. For total discharges greater than critical discharge, the description is developed as were Equations 17 and 21 except that the densities entering both ports must be included as variables. This influences the computation of buoyancy head. The Euler equation must be applied through the top port as it was through the bottom port for critical discharge. That is, the streamline containing the withdrawal density must be chosen. Variables and point locations are defined in Figure 11.

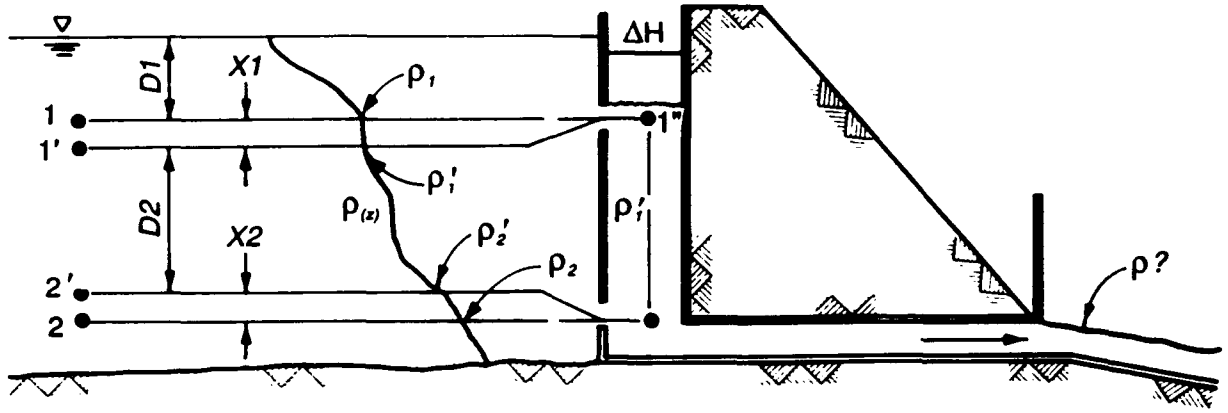

Figure 11. Definition sketch for greater than critical discharge with an arbitrary stratification

59. Once the Euler equation has been applied across both open ports, the previously assumed negligible velocity heads removed, and the pressures hydrostatically evaluated, the resulting equations, for the upper and lower ports respectively, are

$$h1_{1'-3} = D2 + X1 + X2 + \frac{1}{\rho_{1'}}\left[\int_{WS}^{1} \rho(z)\,dz - \int_{1''}^{3} \rho_{1'}dz - \int_{ws-\Delta H}^{1''} \rho(z)\,dz\right] \qquad (28)$$

$$h1_{2'-3} = X2 + \frac{1}{\rho_{2'}}\left[\int_{ws}^{1} \rho(z)\,dz + \int_{1}^{2'} \rho(z)\,dz - \int_{1''}^{3} \rho_{1'}dz - \int_{ws-\Delta H}^{1''} \rho(z)\,dz\right] \qquad (29)$$

where

$D2$ = elevation difference between streamlines containing upper port inflow density and lower port inflow density in the example, m

$X1$ = elevation difference between the upper port center line and the streamline containing the upper port inflow density, m

$\rho_{1'}$ = density entering the upper port, kg/m^3

By an earlier assumption made in conjunction with Equation 21,

$$\Delta H = \frac{1}{\rho_{1'}} \left[\int_{ws}^{1} \rho(z)\, dz - \int_{ws-\Delta H}^{1''} \rho(z)\, dz \right] \tag{30}$$

From this and the logic used in the development of Equation 25, Equations 28 and 29 reduce to

$$h1_{1'-3} = \Delta H \tag{31}$$

$$h1_{2'-3} = \Delta H + \frac{1}{\rho_{2'}} \int_{1}^{2} [\rho(z) - \rho_{1'}]\, dz \tag{32}$$

60. The numerator of the buoyancy head, which is the integral in Equation 32, can be graphically represented as in Figure 12. The small darkened region at the top is negative since the density in the well is greater than the density in the pool for that small distance. The larger shaded region is positive, indicating that the density influences will induce more flow through the lower port. A procedure similar to that used to develop Equations 19 and 22 produces the following relationship among port flows for arbitrary stratification:

$$QT = \sqrt{\frac{2gA_u^2}{k_u} \Delta H} + \sqrt{\frac{2gA_1^2}{k_1} \left\{ \Delta H + \frac{1}{\rho_{2'}} \int_{1}^{2} [\rho(z) - \rho_{1'}] \right\}} \tag{33}$$

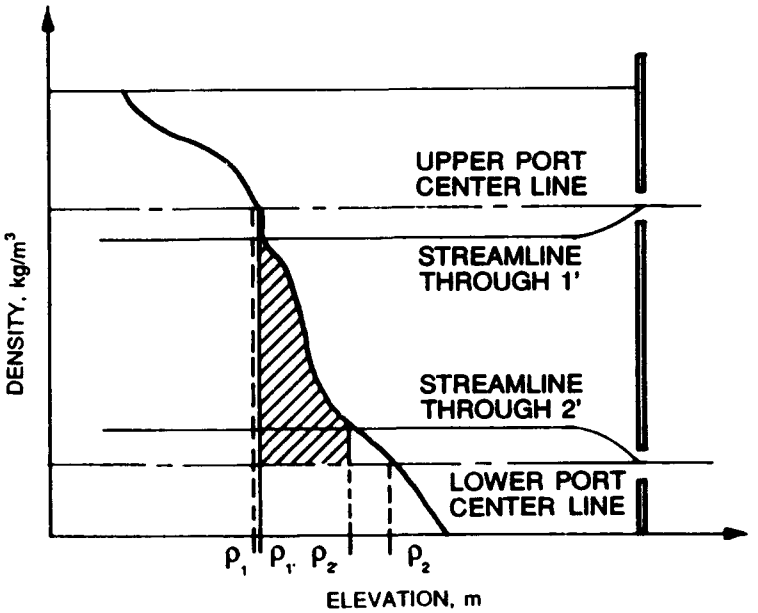

Figure 12. Numerator of the buoyancy head for arbitrary stratification

More Than Two Levels of Withdrawal

61. Often three or more levels of withdrawal are needed simultaneously. This has occurred at reservoir sites where, for the prescribed release quantity, the use of two ports would violate either a maximum port-velocity criterion or a maximum port flow dictated by hydraulic considerations. More than two levels may also be required to provide flexibility in meeting release quality requirements. Figure 13 gives an example of three levels of withdrawal in an arbitrarily stratified pool.

62. Depending upon the stratification, multiple blocked ports and multiple critical discharges may exist, so the term "critical discharge" must be redefined as the discharge above which flow will occur through every open port. The response of the structure in Figure 13 to increasing discharge will be to overcome blockage beginning with the middle port and then the upper port. Quantification of the theoretical critical discharge is similar to that for previous examples. Figure 13 shows the predicted condition of the system at critical discharge.

63. Theoretical critical discharge will occur when the density entering the upper port fills the wet well between the upper and middle ports and the density entering the middle port fills the wet well between the middle and

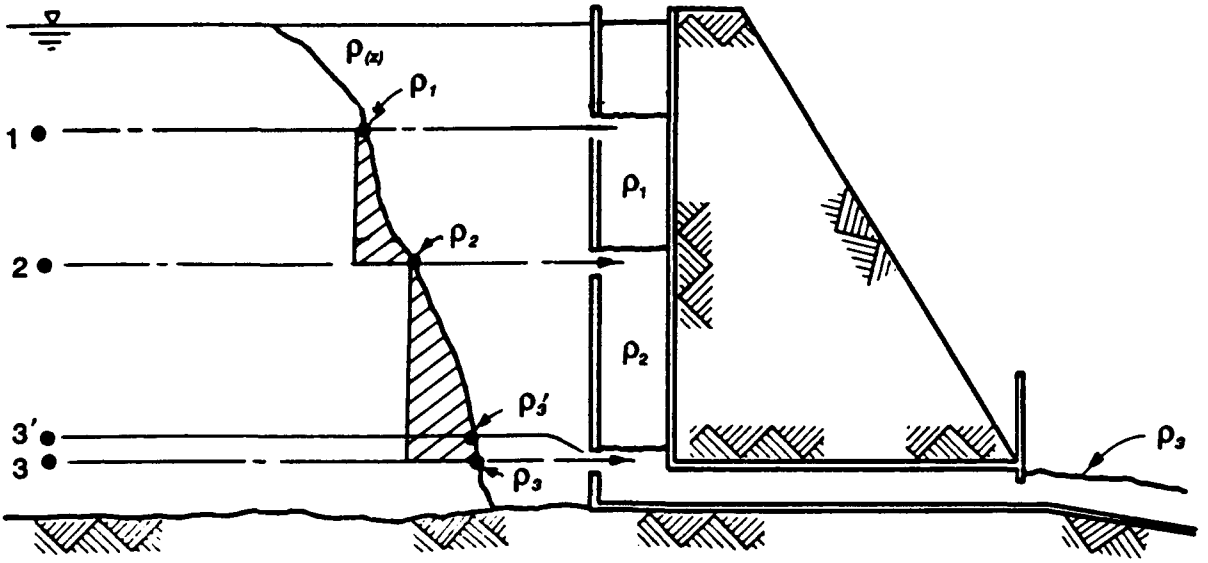

Figure 13. Three levels of simultaneous withdrawal at critical discharge

lower ports. Again, for such extremely low flows, the densities entering the blocked ports are assumed to be the port center-line densities from the pool stratification. Theoretical critical discharge can be found by writing the Euler equation across the lower port between the pool and the well, as before. The resulting formula follows

$$QC = \sqrt{\frac{2gA_1^2}{k_1}\left\{\frac{1}{\rho_2}\int_1^2 [\rho(z) - \rho_1]dz + \frac{1}{\rho_{3'}}\int_2^3 [\rho(z) - \rho_2]\right\}} \tag{34}$$

64. For discharges greater than critical discharge, a few additional considerations are required beyond the two-level work to describe the flow distribution. The density between the middle and lower ports in the wet well will be a function of the flow through each of the ports. Figure 14 shows the example structure at a discharge larger than critical.

65. The buoyancy head for the upper port is zero. The buoyancy head for the middle port is computed as in the arbitrary-stratification case. However, the buoyancy head for the lower port will depend on the flow distribution between the upper and middle ports. The buoyancy head terms are computed

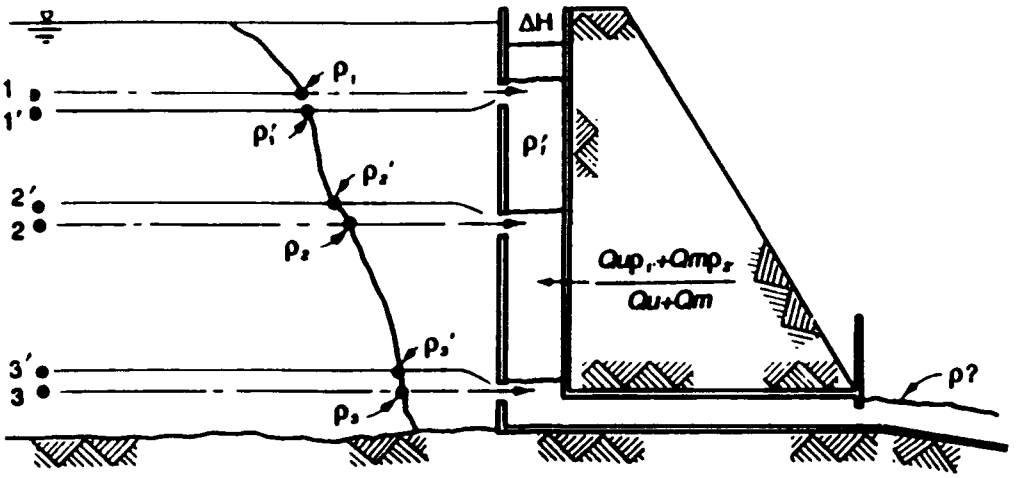

Figure 14. System description at a discharge larger than critical

cumulative downward as shown in Equation 35. The numerators of these terms are shown in Figure 14.

$$BH_u = 0$$

$$BH_m = BH_u + \frac{1}{\rho_{2'}} \int_1^2 [\rho(z) - \rho_{1'}]dz \tag{35}$$

$$BH_1 = BH_m + \frac{1}{\rho_{3'}} \int_2^3 \left[\rho(z) - \left(\frac{QU\rho_{1'} + QM\rho_{2'}}{QU + QM}\right)\right]dz$$

where

BH_u = buoyancy head for the upper port, m

BH_m = buoyancy head for the middle port, m

$\rho_{2'}$ = density entering the middle port, kg/m^3

BH_1 = buoyancy head for the lower port, m

$\rho_{3'}$ = density entering the lower port, kg/m^3

QM = flow rate through the middle port, m^3/sec

66. Quantification of the flow distribution will follow from writing the Euler equation across each of the open ports to the point where the different densities meet. This results in the following equation for flow distribution where

$$QT = \sqrt{\frac{2gA_u^2}{k_u}(\Delta H)} + \sqrt{\frac{2gA_m^2}{k_m}(BH_m + \Delta H)} + \sqrt{\frac{2gA_l^2}{k_l}(BH_l + \Delta H)} \quad (36)$$

where

A_m = area of the middle port, m^2

k_m = loss coefficient for the middle port

Extension of the theory to more than three levels of withdrawal produces the following equation in which each term in the summation represents the individual port flow for level i .

$$QT = \sum_{i=1}^{n} \sqrt{\frac{2gA_i^2}{k_i}(BH_i + \Delta H)} \quad (37)$$

where

n = number of open port levels

A_i = area of port level i , m^2

k_i = head-loss coefficient for port level i

BH_i = buoyancy head for port level i , m

67. Equation 37 is theoretically applicable to any number of withdrawal levels for any stratification. The solution is iterative on ΔH with a required selective-withdrawal calculation for each estimate of inflowing density for each of the individual port flows.

68. The procedures and equations presented in this part and Part IV will be referred to as the stratified-flow-distribution (SFD) algorithm.

Algorithm Assumptions

69. The complete description of simultaneous, multiple-level withdrawal in a single-flow-control intake structure would entail the modeling of 3-D, turbulent flow. The use of the Euler equation to simplify the analysis required that several assumptions be made, as follow:

a. The fluid is assumed to be incompressible. This assumption is valid for reservoir intake structures, because the change in water density because of acceleration or deceleration is very small.

b. The points of integration for the Euler equation are assumed to lie on a common, smooth streamline. The flow is assumed irrotational between the points of integration. Turbulence resulting from flow entering the wet well may prevent the establishment of smooth streamlines from the pool to the wet well and the meeting of the streamlines from each port in the well. An estimate of the impacts of this assumption on the accuracy of the SFD algorithm is reserved for comparison with observed data in Part V of this report.

c. Frictional losses in the well between the open-port levels were assumed negligible. Flow entering an intake structure undergoes a sudden contraction followed generally by a sudden expansion. These losses are significantly larger than the losses due to skin friction as flow passes through the wet well. Miller (1978) makes a similar observation for inlet manifolds.

d. The in-well stratification above the highest port is also assumed equal to that of the pool, with the only difference being the water surface differential between the pool and well. Some mixing will occur in the well above the highest open port. However, from the hydrostatic pressure assumption, the pressure drop across the uppermost open port is the same as the pressure drop resulting from the assumption of no mixing, making this assumption valid.

e. The head-loss coefficients are assumed to be given directly or to be obtainable. These coefficients include the losses associated with contraction and expansion of the flow passing through the intake ports, the impingement of the velocity jet on the wet-well walls, and the generation of eddies in the well. The structural configuration for the single well with multiple ports resembles a series of tee connections in a pipe system. The loss coefficient for a tee is partly dependent on the cross flow in the tee (Miller 1978). Applying this to the single wet well, the loss coefficient of the lower port should depend on the flow rate through the upper port. Additionally, ports come in many sizes and shapes, the thickness of the walls vary, and trash control devices in front of the ports are different from structure to structure. In other words, finding the appropriate loss coefficients is no simple task. In the equations, however, for flows not near critical discharge, the relationship among the loss coefficients is more important than the absolute coefficient in predicting flow distribution.

f. Lastly, it has been assumed that no hydraulic conditions exist in the wet well which would prevent the establishment of stable flow patterns. An example of an adverse hydraulic condition, proposed but never observed, is called hydraulic blockage. Theoretically, at discharges much higher than critical discharge, the turbulent velocity jet entering the lower port may block flow from the upper port. Difficulties of this kind would need to be handled on a case-by-case basis.

70. The effects of the velocity jet on the critical discharge have not been described. Therefore, the theoretical critical discharge given by the

SFD algorithm represents a conservative estimate of the actual critical discharge. In practice, this causes no difficulty, because the operation of multiple ports very near the critical discharge is seldom an attractive operational scenario. A very similar release quality could be achieved by closing the theoretically blocked ports.

71. For discharges greater than critical, the velocity jet continues to have an effect. That is, a fraction of the distance between the open ports in the well will be filled with water from the lower port. Comparison with observed data will indicate whether or not this phenomenon is important.

PART IV: SPECIAL CASE APPLICATIONS

72. The portion of the SFD algorithm proposed in Part III is applicable to many structures for which simultaneous, multiple-level withdrawal is needed. Extensions include "inverted" structures, structures that can partially close the intake port gates, and structures with multiple wet wells.

Inverted Structure

73. In most reservoir intake structures, the wet-well outlet is at or below the lowest intake port. However, at least one CE-operated single-wet-well intake structure has intake ports below the wet-well outlet. In Figure 15, the wet-well outlet is at the same elevation as the upper port. Otherwise, it is identical to the structure in Figure 5.

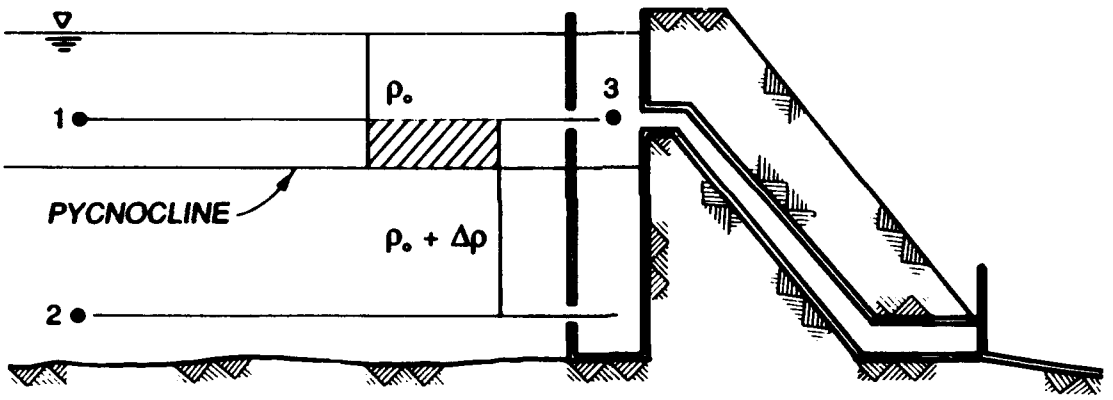

Figure 15. Wet-well outlet at the elevation of the upper ports

74. Analysis of this configuration with the Euler equation is similar to that for previous applications, and the head-loss relationship between the ports is

$$h1_{2\text{-}3} = h1_{1\text{-}3} - \frac{\Delta\rho D2}{\rho_o + \Delta\rho} \tag{38}$$

The buoyancy head again contributes to the lower port head loss. However, as shown in Equation 38, the buoyancy head will have a negative value. Buoyancy forces produce a greater flow rate through the upper port than that for the

homogeneous density condition or the condition in Figure 5 because additional energy is required to pull the heavier water upward in the wet well. The addition of a negative buoyancy head to the lower port accounts for the additional energy by hindering flow through the lower port. This has led to a more general method of computing buoyancy head for a wet-well outlet at any elevation. The buoyancy head for arbitrary stratification becomes

$$BH_i = BH_{i-1} + \frac{1}{\rho_i} \int_{i-1}^{i} [\rho(z) - \rho_w] dz \tag{39}$$

where

i = port index beginning with the highest port and proceeding downward (as integration limits, these are port elevations, m)

ρ_i = density entering port level i, kg/m^3

ρ_w = density in the wet well between port levels i and $i-1$, kg/m^3

75. For an outlet located between the open-port elevations, the buoyancy head computations must be made between each inlet and outlet in the wet well, as explained below using the linear stratification example (Figure 16) for reference.

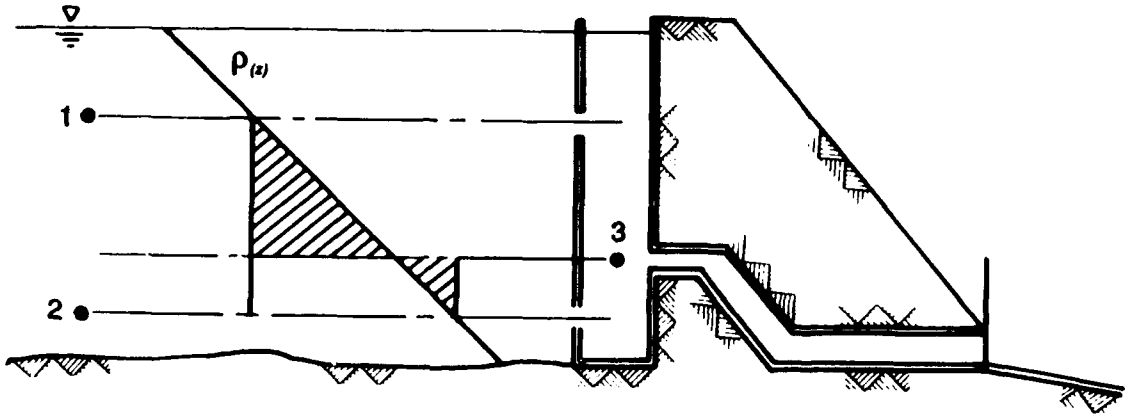

Figure 16. Wet-well outlet between the open-port elevations in a linear stratification

76. Most of the flow for this case will pass through the lower port since integration of Equation 39 between the open-port elevations produces a positive buoyancy head for addition to the lower port. In Figure 16, shaded

areas to the right of the density profile correspond to negative buoyancy heads and those to the left correspond to positive buoyancy heads.

Effects of Intake Port Gate Throttling

77. The ports of some intake structures are equipped with gates that may not necessarily be operated in the customary mode of fully open or fully closed. Since the head loss across these ports depends on the gate opening and since the losses strongly affect the flow distribution among the ports, an investigation of the effects of partial intake gate closure (throttling) is warranted.

78. Throttling, as it is used herein, is insufficient to transfer flow control to the intake ports, so flow control remains downstream. By partially closing the lower port, the area is reduced, the velocities and head loss are increased, and consequently, the lower port portion of the total discharge is reduced. Therefore, by manipulating the head losses through throttling of selected ports, control is gained over the flow distribution among the open ports.

79. The effects of port throttling on the flow distribution are best illustrated by example, for which the conditions in Figure 5 will be used. Assuming for illustration that the ports have equal areas and loss coefficients, that the loss coefficients do not vary with gate opening, the graph in Figure 17 results for a two-layer stratification.

80. The dashed curve in Figure 17 represents the flow distribution for both intakes fully opened. The solid curve to the right and below the dashed curve represents the upper port throttled 50 percent and the lower port fully open. The solid curve to the left and above the dashed curve represents similar throttling for the lower port and the upper port fully open. Each curve asymptotically approaches the flow distribution that would occur in a homogeneous density environment represented by the horizontal lines. The vertical axis gives the upper port flow contribution to the total discharge, which is shown on the horizontal axis. The discontinuity along the line for no flow through the upper port identifies theoretical critical discharge. Theoretically, for all equal or lesser flows, the entire discharge passes through the lower port.

81. These curves demonstrate that throttling the lower port gate significantly affects the critical discharge. However, throttling of the upper

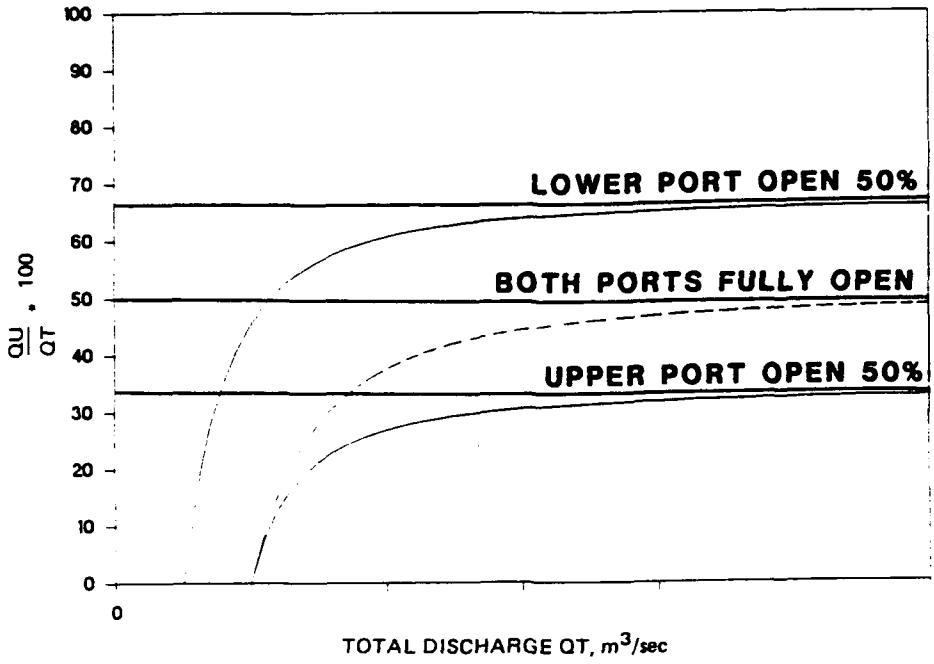

Figure 17. Effects of port gate throttling

port gate does not affect the critical discharge since no flow enters the upper port with buoyancy blockage. Assuming unlimited control of intake port gates, it can be shown by extrapolation that any distribution of flow is theoretically attainable.

82. Limited ability to throttle intake port gates will exist in practice. Even if the ports have been designed to accommodate throttling, factors such as gate vibration, excessive intake port velocities, cable stretching, and imperfect controlling devices will limit the minimum gate setting.

Multiple-Wet-Well Structure with Common Flow Control

83. Multiple-wet-well structures with single-flow-control points operate much like single-wet-well structures and are subject to stratification influence on flow distribution. Many dual-wet-well structures that have been retrofitted with hydropower and tuning-fork designed structures such as that in Figure 18 fall into this category.

84. Many of the assumptions as in the previous work apply here, and buoyancy blockage remains a problem. The well with the higher open port (well number 1 in the example (Figure 19)) is potentially subject to buoyancy

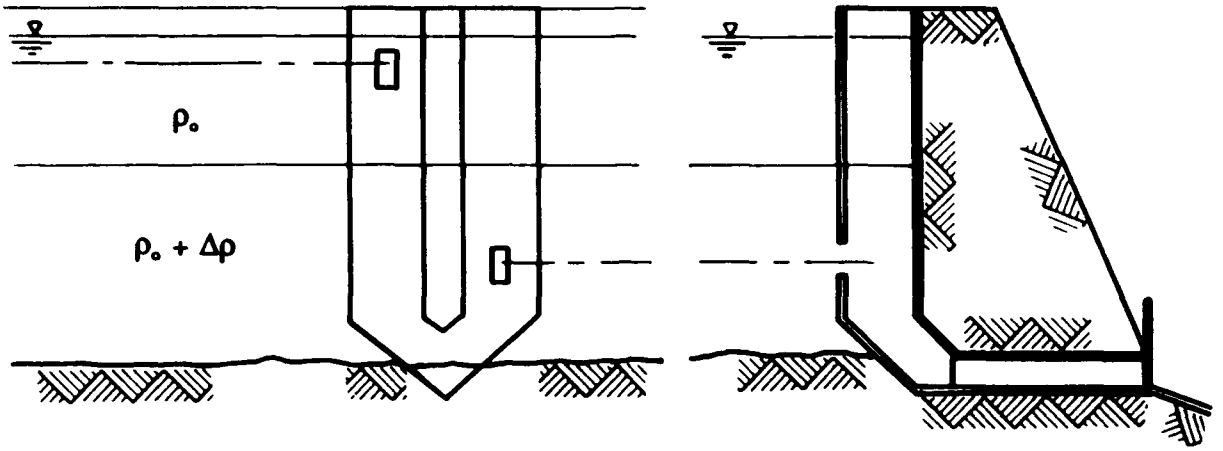

Figure 18. Multiple wet-well structure in a two-layer stratification

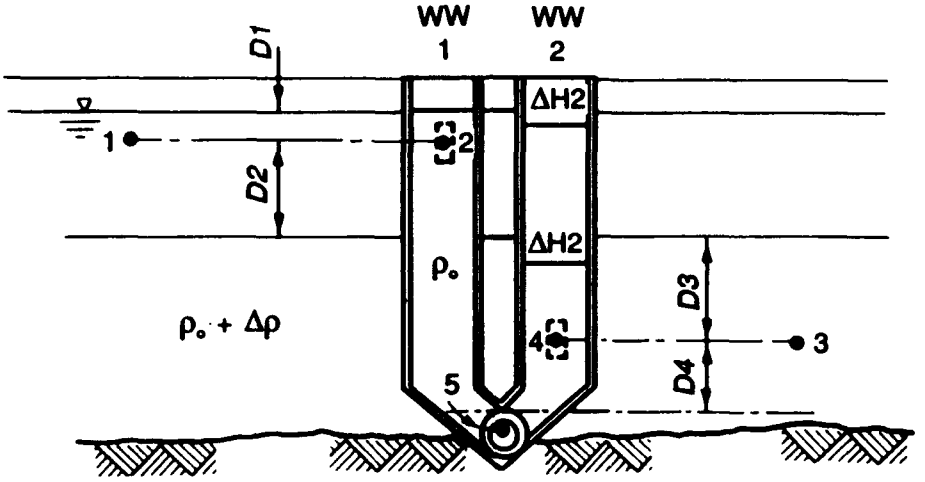

Figure 19. Theoretical critical discharge for a tuning-fork structure in a two-layer stratification

blockage. Figure 19 shows the theoretical critical discharge condition for the example structure and stratification.

85. Integration of the Euler equation in well number 2 at critical discharge gives

$$h1_{3-4} + h1_{4-5} = \frac{(D3 + D4)\,\Delta\rho}{\rho_o + \Delta\rho} - \frac{V_5^2}{2g} \qquad (40)$$

where

hl_{3-4} = head loss from entrance into well, m

hl_{4-5} = head loss from flow passage in the well between the port elevation and that elevation where the waters meet, m

$D3$ = elevation differences between the pycnocline and the lower port center line, m

$D4$ = elevation difference between the lower port and the point of mixing, m

V_5 = velocity of the fluid at point 5, m/sec

86. The hydrostatic assumption applies only between points 3 and 4 inclusively. From point 4 to point 5, the pressure is considered to be non-hydrostatic. At critical discharge, wet well 2 has no flow, and the hydrostatic assumption is appropriate in that well.

87. Above critical discharge, the following head-loss relationship results from integration of the Euler equation

$$hl_{3-5} = hl_{1-5} + \frac{(D3 + D4)\Delta\rho}{\rho_o + \Delta\rho} \tag{41}$$

where

hl_{3-5} = head loss from point 3 to point 5, m

hl_{1-5} = head loss from point 1 to point 5, m

88. Extension of these equations to arbitrary stratification gives the same result as for the single wet well, except for an additional buoyancy term. Adopting the same prime conventions for variables as in Part III (where primes denote the streamlines containing the density entering the port), the head-loss description for flows larger than critical is

$$hl_{3'-5} = hl_{1'-5} + \frac{1}{\rho_{3'}} \left\{ \int_1^3 [\rho(z) - \rho_{1'}] dz + (\rho_{3'} - \rho_{1'}) D4 \right\} \tag{42}$$

89. The integration of $\rho(z) - \rho_{1'}$ only extends down to point 3, indicating that the stratification beneath the lowest port is irrelevant except for its effect on the density entering the lower port. The last term in Equation 19 describes the effect of moving the point of mixing from the lowest

port in the single-well case to the juncture of the two wet wells in this case. Conversion from a head-loss relationship to one of discharge would be similar to the procedure for Equation 36.

PART V: COMPARISON OF SFD-ALGORITHM PREDICTIONS WITH OBSERVED DATA

90. In Part V, predictions of the SFD algorithm developed in Parts III and IV are compared with laboratory and field data to evaluate their accuracy.

91. Initially, the response of a simple structure to increasing flows, as theorized in conjunction with Figure 5, was evaluated qualitatively. A visual laboratory experiment was undertaken, using an approximately two-layer stratification produced with saline and fresh water. The upper layer was dyed to enhance the interface visibility.

92. Prior to initiation of flow from the simplified model intake structure, stratification was virtually identical in the wet well and the reservoir. When a small flow was initiated, the pycnocline in the wet well dropped slowly to a stable elevation. As the flow was slightly increased, the pycnocline reached a lower equilibrium position. When the pycnocline was lowered to approximately 0.3 m above the lower port, the jet through the lower port began to disturb the sharp interface in the wet well. Small amounts of the dyed surface water mixed with the clear water entering the lower port and exited the structure.

93. Under larger release conditions, flow passed through each of the ports. Flow in the well near the lower port was turbulent, but stable. These laboratory observations compared well with the theorized response of a structure to increasing discharge.

Two-Layer Stratification

94. Quantitative evaluation of the algorithm's accuracy began with a simple case. A structure with two ports in a two-layer density stratification (Figure 5) was tested in the laboratory. Two separate testing sequences were conducted in a Plexiglas-constructed, general model of an intake structure whose face was mounted flush with a vertical wall (Figure 20).

95. The model well's interior dimensions were 0.15 m wide, 0.15 m deep, and 1.22 m tall. The intake ports, each 0.064-m-diam circular orifices cut in the 0.013-m-thick Plexiglas walls, were located with centers 0.15 and 1.07 m above the bottoms of the flume and wet well. The model reservoir's surface area exceeded 70 m^2, which prevented significant water surface or

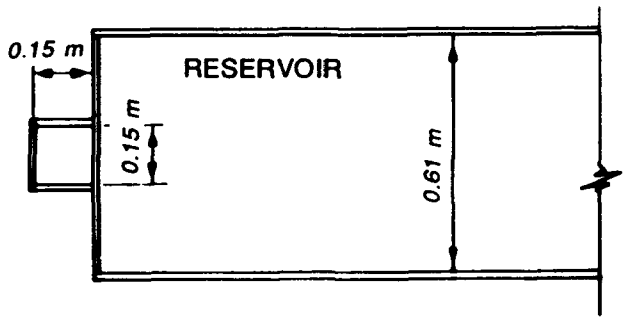

a. Plan view

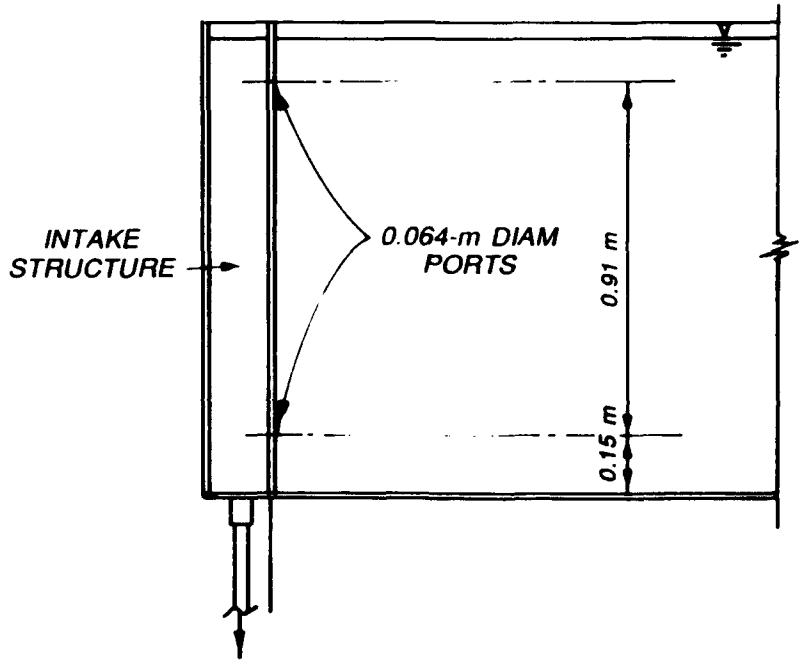

b. Elevation view

Figure 20. Schematic of the test facility

stratification changes during any single test, even though the water withdrawn was not replaced.

96. Density stratification in the test flume was composed of a saline-water hypolimnion and a freshwater epilimnion. The sharp pycnocline was achieved by introducing the fresh water slowly over a broad-crested weir at the desired elevation of the interface.

97. Individual port flow rates were measured indirectly in both testing sequences. In the first testing sequence, conducted by Tate and Dortch,* the lower layer was tagged with fluorescent dye. Flow distribution was deduced by measuring fluorescence of the release water. In the second testing sequence, conducted as a part of this investigation, the individual port flow rates were deduced by measuring the release density. The total discharge was monitored in each case to facilitate the computation of port flows.

98. The analyses for both testing sequences focused on the measured values of upper port flow in comparison with the predictions of the algorithm. The lower port could as easily have been chosen. For two open ports with equal head-loss coefficients, Equations 18 and 19 lead to the following equation for upper port flow:

$$QU = \frac{k_1 QT^2 - BH_1 2g A_1^2}{2k_1 QT} \tag{43}$$

where the terms are the same as defined in Part III.

99. The only unknowns in Equation 43 that must be obtained are the loss coefficient and the buoyancy head. The loss coefficient developed by Tate and Dortch* accounted only for the losses through the orifice. The losses associated with the velocity-jet impingement and eddy development in the well were not included. To include these effects in the loss coefficient, the algorithm was employed for one of the tests with a high discharge such that the density influences should have been minimal. The loss coefficient obtained was 2.7.

100. The buoyancy head was computed from the density difference between the two layers and the elevation difference between the lower port center line and the pycnocline.

101. A comparison between the laboratory measurements by Tate and Dortch* and the predictions from Equation 43 is given in Figure 21. These tests included several stratifications and discharges, so the plots have been made nondimensional. The ordinate is total discharge (QT) divided by theoretical critical discharge (QC), and the abscissa is stratification-influenced upper port flow (QU) divided by the upper port flow expected for a uniform

---

* Op. cit.

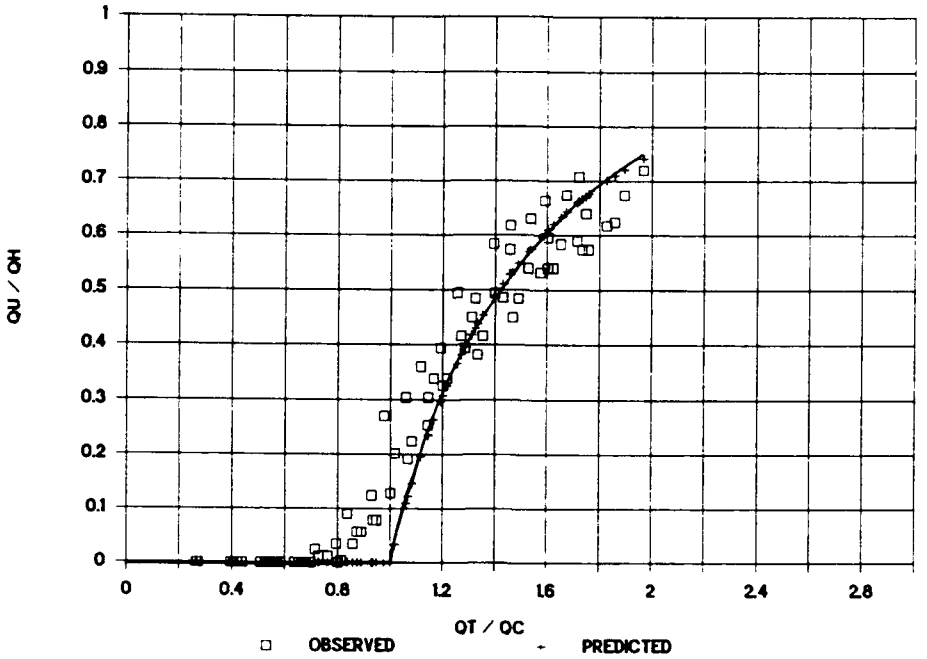

Figure 21. Predictions and Tate and Dortch observations (unpublished data) in a two-layer stratification

density (QH). These nondimensional values produce a single curve for predictions, regardless of the stratification.

102. A value of unity for QU/QH indicates that flow through the upper port equals that predicted when stratification influences are absent. In a density-stratified pool, this point will be approached asymptotically as the total discharge is increased. For this set of tests, the upper port flow remained less than 75 percent of the homogeneous-pool, upper port flow. The total discharge never exceeded twice the theoretical critical discharge.

103. General agreement between the predictions and observations is very good with the standard error of estimate (Steel and Torrie 1960) of the upper port flow percentage at 3.6 percent.

104. Significant discrepancies between the predictions and observations are, for the most part, confined to total discharges between 85 and 110 percent of theoretical critical discharge. The upper port contribution is consistently and substantially underpredicted for $QU/QH < 0.25$. In practice, operation at a discharge close to critical discharge will seldom be attractive since the release quality will very closely resemble that through the lower port.

105. Similar results from the second testing sequence, using the same loss coefficient, are presented in Figure 22 with the same conventions as in the previous example.

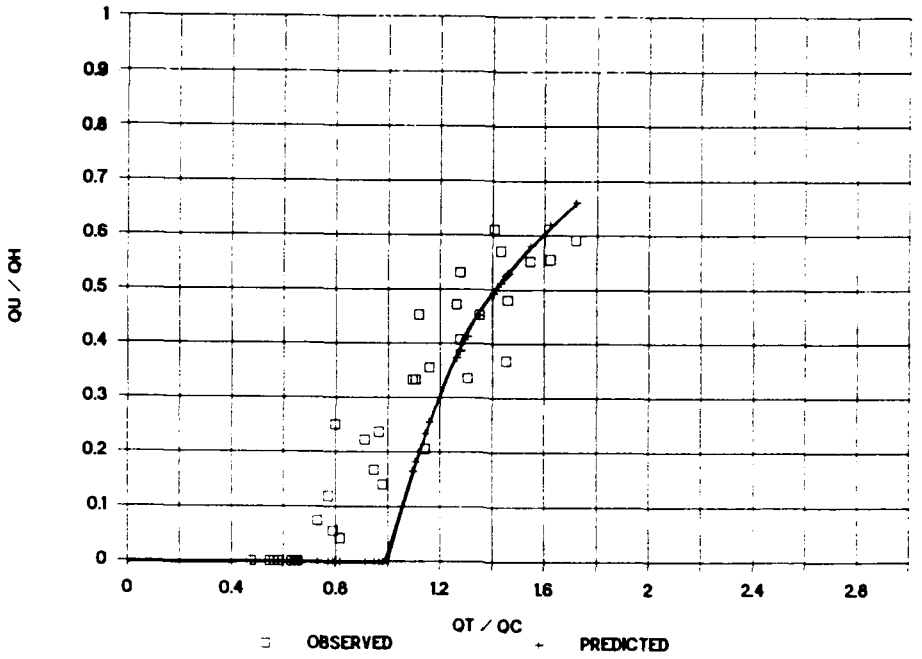

Figure 22. Predictions and observations from the second sequence in a two-layer stratification

106. Again large errors occurred for discharges between 85 and 110 percent of theoretical critical discharge, but additional large errors were observed at discharges between 60 and 85 percent of theoretical critical discharge. Overall, the agreement is good with the standard error of estimate for the fraction of flow through the upper port at 4.6 percent.

107. Sources of discrepancies between predictions and observations for both testing sequences may include inaccurate loss coefficients and the in-well effects of the lower port velocity-jet impingement. A uniform increase in the loss coefficient would produce better correlation near critical discharge, but poorer correlation elsewhere. The loss coefficient for the lower port may not be a constant, as assumed, but may vary with the amount of flow from the upper port as suggested by Miller (1978) and detailed in Part III. Insufficient data were available to examine this contention.

108. The computation of buoyancy head for the two-layer stratification was likely not a significant source of error as the densities in each port were estimated with confidence. A more likely source of error is the velocity

jet entering the lower port. As previously stated, the mixing region associated with this jet may cause the release of water from the upper port at a discharge less than the theoretical critical discharge. That would account for the errors in prediction near theoretical critical discharge.

Linear Stratification

109. The test facility used in the two-layer stratification testing was also used to verify the SFD algorithm for linear stratification. To achieve an approximately linear stratification, controlled mixing with small, submersible pumps was used. The loss coefficients developed during the two-layer work were adopted since no physical changes to the test facility were made. Determination of the buoyancy head was, however, not as straightforward as suggested in Equation 21. The intermediate flow assumption was violated for all tests. Therefore, the density entering each port was adjusted according to existing selective withdrawal descriptions for boundary interference as developed by Smith et al. (1987). The resulting comparison between predictions and observations for linear stratification is provided in Figure 23.

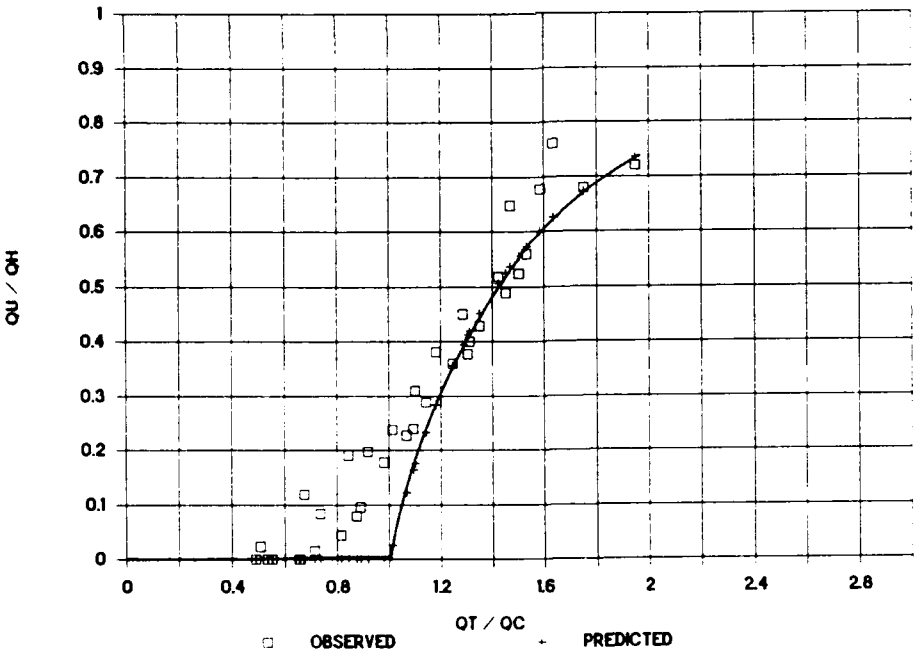

Figure 23. Predictions and observations in a linear stratification

110. The error trends follow closely those described in the two-layer comparison; the largest errors occur near critical discharge. The standard error of estimate for the upper port contribution to the total discharge was 6.5 percent. The error sources identified in the two-layer comparison (inaccurate loss coefficients and lower port velocity-jet influences) were also of potential concern for the linear stratification comparisons.

Arbitrary Stratification

111. Additional tests were conducted to verify that Equation 33 would adequately apply for the two-port, no throttling, single-wet-well case for arbitrary stratification. Field data were collected at Taylorsville Dam, Kentucky. The intake structure there has two wet wells, but, during this study, the wells were often operated individually as single wells. The structure has five 1.83- by 1.83-m intake ports in each wet well. These intake ports were operated either fully opened or fully closed, with invert elevations of 153.3, 157.9, and 162.8 m.* Each wet well was about 4.57 m deep, 3.35 m wide, and 16.15 m tall.

112. Since all the observations were made within a few days, the stratification in the reservoir remained fairly constant. The observed thermal stratification was converted to density stratification. Flow through each of the open intakes was measured with a series of velocity probes mounted on moveable racks.

113. A few of the observations were made with multiple intakes open at the same elevation and other intakes closed. These observations provided no useful information about the influence of density stratification on flow distribution, but they did provide information about loss coefficients.

114. The water temperature entering each port was also measured and converted to density. The buoyancy-head terms followed from Equation 39. Since the port head-loss coefficients were not equal, the use of Equation 43 to determine upper port flow was not possible. However, Equations 18 and 19 produce the following equation relating the upper port flow to the total discharge, the port areas and loss coefficients, and the buoyancy head

---

* All elevations cited herein are in metres referred to the National Geodetic Vertical Datum (NGVD).

$$QU^2\left(\frac{k_1}{A_1^2} - \frac{k_u}{A_u^2}\right) - QU\left(\frac{2k_1QT}{A_1^2}\right) + \frac{k_1QT^2}{A_1^2} - BH_1 2g = 0 \qquad (44)$$

From this equation, the upper port flow can be computed using the quadratic formula when the losses and port areas differ.

115. Dividing Equation 44 by the homogeneous-upper-port flow prediction produces the following ratio for QU/QH , for all $QT > QC$:

$$\frac{QU}{QH} = \frac{1 - \sqrt{1 - \frac{A_1^2}{k_1}\left(\frac{k_1}{A_1^2} - \frac{k_u}{A_u^2}\right)\left(1 - \frac{QC^2}{QT^2}\right)}}{1 - \sqrt{1 - \frac{A_1^2}{k_1}\left(\frac{k_1}{A_1^2} - \frac{k_u}{A_u^2}\right)}} \qquad (45)$$

Plotting QT/QC versus QU/QH no longer produces a single line of predicted values since the term

$$\left(\frac{k_1}{A_1^2} - \frac{k_u}{A_u^2}\right) \neq 0 \qquad (46)$$

creates diversity even among tests that have the same values of QC/QT .

116. Figure 24, which shows the comparison between predictions and observations for the Taylorsville single-well tests, demonstrates the variability of the predictions.

117. Figure 24 shows the predictions and observations for a single well. The disagreement encountered at about 95 percent of theoretical critical discharge was anticipated from earlier comparisons. The correlation is acceptable with a standard error of estimate of 3.0 percent in the predicted division of the flow. Sources of error for this data set are not immediately obvious if the observed information is assumed to be accurate.

118. The SFD algorithm compared well with the observations made in two-layer, linear, and arbitrary stratifications with two ports open. Discrepancies between predictions and observations occurred consistently near critical discharge when the upper port flow was underpredicted. Since operations in the range of flows near critical discharge will not be often selected in

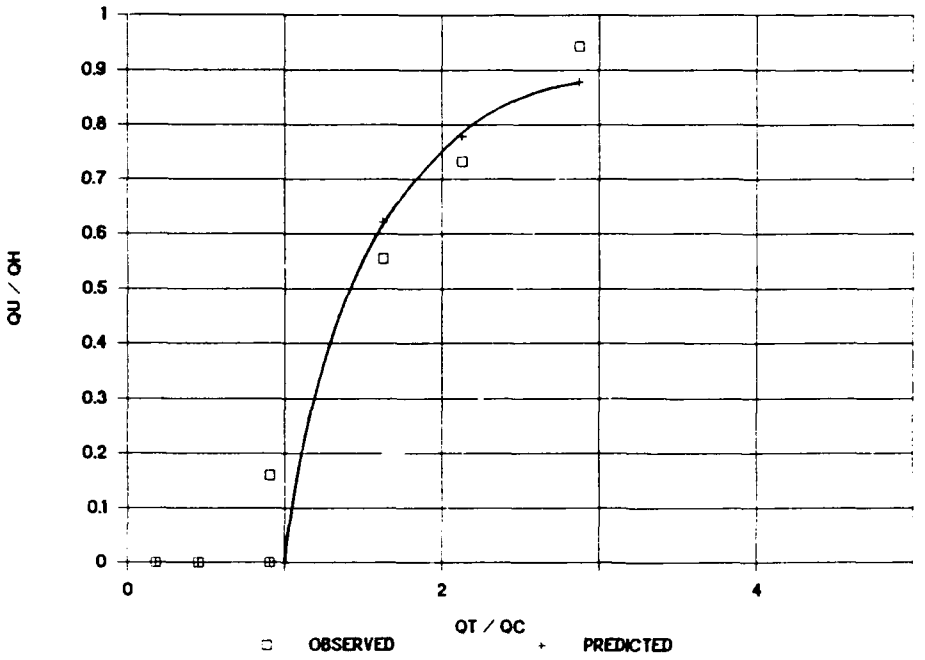

Figure 24. Taylorsville Dam single-well predictions and observations

practice, these results were considered acceptable, and more complex problems were examined.

Three or More Levels of Withdrawal

119. Data collected from the 1:80 scale physical model of the Lost Creek Dam, Oregon, reservoir intake structure were compared with SFD-algorithm predictions for three or more simultaneous levels of withdrawal. The prototype Lost Creek intake structure contains 11 intake ports that are 2.44- by 4.57-m and a turbidity intake conduit. These 12 intakes enter a single, 9.14-m-diam wet well (3 intakes per level) over a vertical distance of 80 m.

120. Two regulating outlets and one hydropower penstock withdraw water from the single wet well. Intake-port gates are operated fully open or fully closed. Minimum flow through the prototype structure is 19.8 m^3/sec, so lesser discharges were not examined in the model study (Howington 1989).

121. Stratification was simulated by various water salinities. A large number of stratification conditions were tested in the model to represent the potential conditions at the prototype. Two to four levels of simultaneous withdrawal were tested. Selected individual port flows were measured with

calibrated velocity probes. Head-loss coefficients were determined for each model intake port. Additional information concerning the testing procedures can be found in the model-study documentation by Howington (1989). The buoyancy head was determined using the site-specific selective withdrawal description developed as part of the intake structure analysis.

122. Equation 37 was solved iteratively to predict port flows. Comparison between predictions and observations could not be presented in the format of Figures 21-24, since individual flows were not measured for each open port and three or more ports were often open. Therefore, the predicted and observed percentages of total discharge passing through that port measured for each test are plotted in the manner shown in Figure 25.

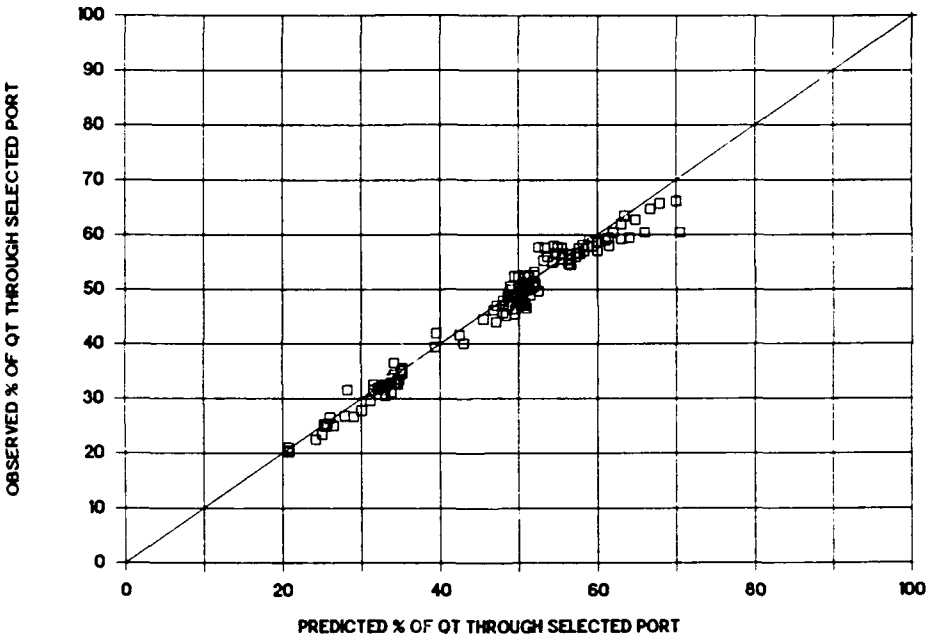

Figure 25. Predicted versus observed percentages of total discharge in the Lost Creek model

123. The agreement is excellent, with only one data point demonstrating an error in excess of 10 percent of the total discharge. The diagonal line in the figure represents perfect agreement between the predictions and observations. It should be noted that the flow percentages tested never exceeded 75 percent and never fell below 20 percent of the total structure discharge. Thus, the previously identified inaccuracy near critical discharge was not encountered with this data set. The high flow rates and related high head

losses prevented the establishment of buoyancy blockage for any of the test conditions.

Inverted Structure

124. The Lost Creek hydropower penstock withdraws water from the wet well above the elevation of the lowest three intakes, creating an inverted structure like that discussed in Part IV. A test from the model study that used one of these low intakes with the hydropower operating was selected as an example. Two ports were open--one above the penstock elevation and one below. Buoyancy head calculations were made with Equation 39. The resulting predictions and observations are given in Figure 26.

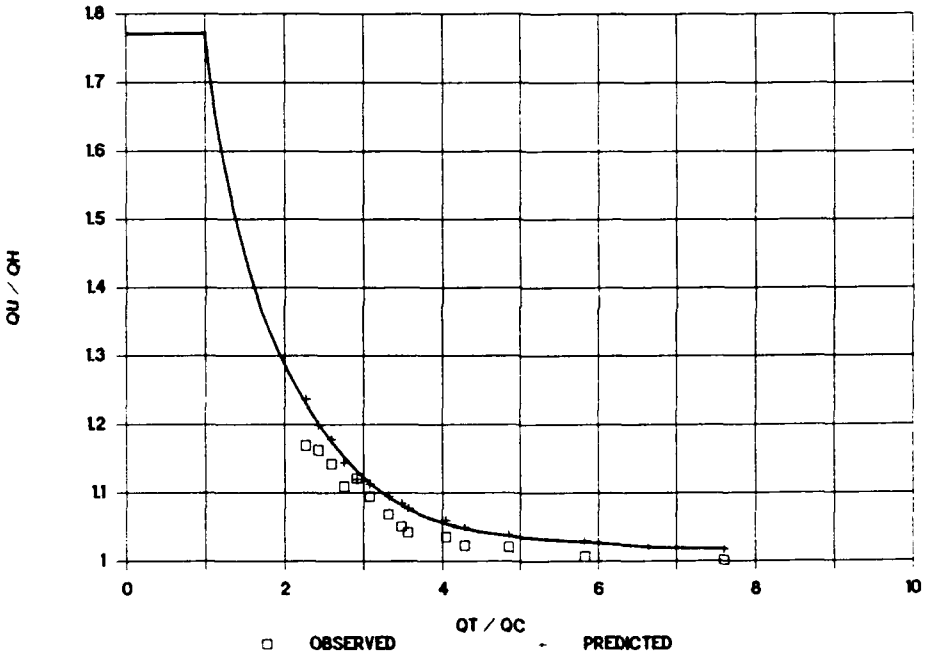

Figure 26. Sample of inverted problem from the Lost Creek Dam data

125. The penstock was located nearer to the higher port, resulting in more energy expended to pull the heavy water up from the lower port than to pull the lighter water down from the higher port within the wet well. Blockage for this test was predicted to occur at 1.77 *QU/QH* when all the flow passed through the higher, not the lower, port.

126. The predictions and observations appeared to approach asymptotically the uniform-density flow distribution (*QU/QH* = 1.0) as the total

structure discharge increased. The effects of density for this test were negligible (less than 5-percent difference between the density-influenced and the homogeneous upper port portion of the total discharge) at a total discharge of 5 times the critical discharge. The upper port flow was very slightly overpredicted for all observations, but the agreement between predictions and observations is still good.

Partial Intake Port Gate Closure

127. Several sources of data were available in which partial port gate closure (throttling) was used to control the flow distribution among the open intakes. Testing of the Warm Springs Dam in California and the Applegate Dam in Oregon provided prototype data, while investigation of the 1:20 scale model of the Elk Creek Dam intake structure provided physical model data.

128. The Warm Springs Dam intake structure is composed of three long 1.52-m-diam concrete conduits that extend from the reservoir at invert elevations of 107.29, 119.18, and 131.37 m to a single, 1.83-m-diam steel wet well. Each conduit includes a bend and a horizontally mounted, 1.52-m butterfly valve to control the flow.

129. Field testing at Warm Springs continued for only a few consecutive days, so one reservoir temperature stratification was used for the entire testing sequence. Individual port flows were not measured directly. However, in-conduit temperatures and release temperatures were measured, and only two ports were operated at a time, making the computation of individual port flows straightforward.

130. Accurate description of the losses necessarily included the variation in loss coefficient with gate setting. One set of the tests was set aside for use purely in the determination of loss coefficients. It was assumed that the SFD algorithm would apply for these tests; the loss coefficients needed to complete the equations were then derived. In-well temperature profiles were also collected, permitting the simple and accurate prediction of the buoyancy head.

131. Equation 44 was applied to the collected information, and the algorithm results are plotted against the observations in Figure 27.

132. The predictions compare well with the observed values with the standard error of estimate in flow distribution at 7.0 percent. The

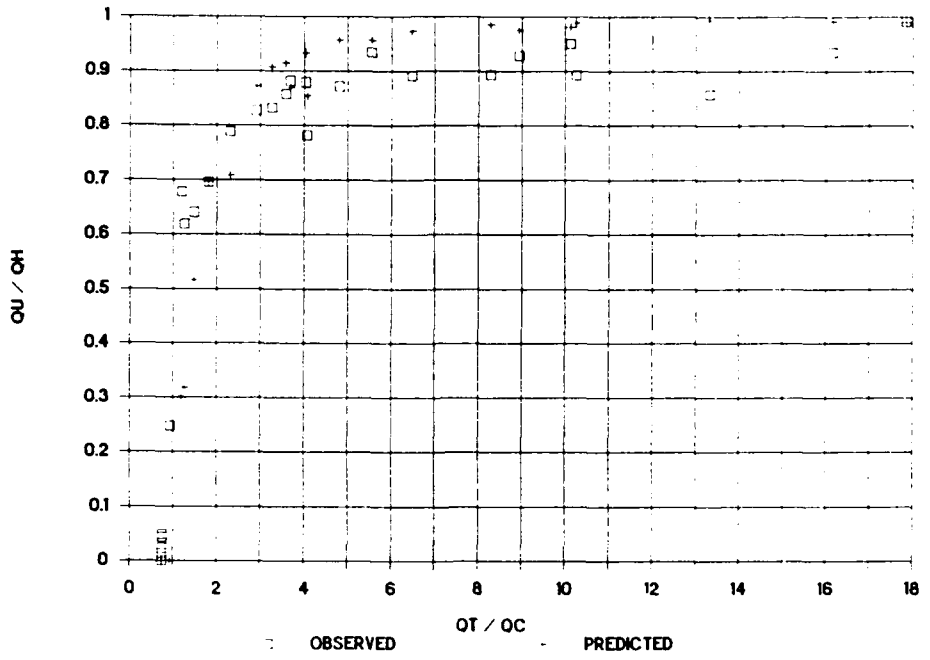

Figure 27. Predictions and observations from the Warm Springs Dam field study

comparisons shown do not include the tests used to derive the loss coefficients. The predicted upper port contributions are generally too high. The discrepancy may arise from the method used in the computation of loss coefficients, which may have created a bias. It appears that the loss coefficients were either slightly too large in general or the upper port coefficient was disproportionally small compared with the lower port. Again the predicted effect of density became insignificant for flows greater than 5 times the critical discharge.

133. To demonstrate the consequences of such errors on the predictability of release quality such as temperature, predicted and observed temperatures for Warm Springs are shown in Figure 28.

134. Only for three tests is the difference between the predictions and observations greater than 1° C, demonstrating that the errors seen in Figure 27 are acceptable in the prediction of release temperature.

135. The Applegate Dam intake structure is a dual-wet-well, dual-flow-control, multiported structure. The US Army Engineer District (USAED), Portland, has conducted a limited series of tests to demonstrate that flows from two ports will blend in a single wet well and that the distribution of flow is controlled by throttling the intake ports. The intakes used in this field

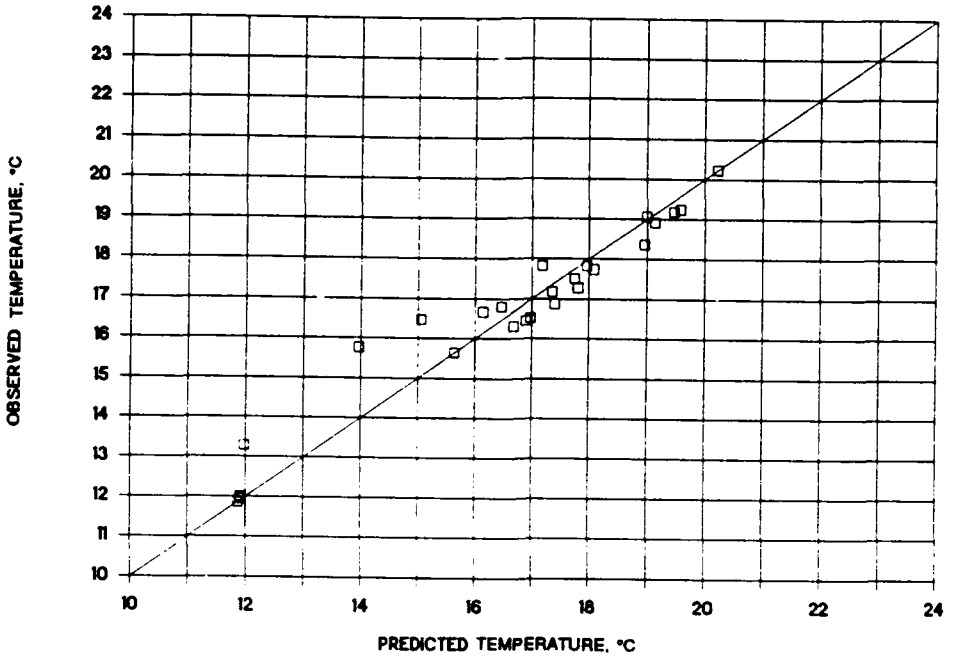

Figure 28. Predicted versus observed release temperatures for Warm Springs Dam

exercise were 1.5 m wide and 1.8 m tall at invert elevations of 588.3 and 560.2 m.

136. Loss coefficients were computed from a few of the prototype observations. These observations were then removed from the data set. For the remaining observations, port flows were determined from the selective-withdrawal-estimated port temperatures, the observed release temperatures, and continuity arguments. Equation 44 was used to predict upper port flow, and the resulting comparison is given in Figure 29.

137. The range of flows used in the Applegate tests was very limited. The lowest *QT/QC* ratio examined was about 6, which corresponded to the smallest gate opening tested for the lower port. Although agreement between predictions and observations is good, with a standard error of estimate of upper port contribution at 4.5 percent, this comparison does not significantly increase confidence in the algorithm's capabilities to predict density influences since their effects were minimal. It does, however, support the proposal that blending of different water densities will occur in single wet wells.

138. Release temperatures are plotted against the predictions in Figure 30. The temperature predictions were all within 1° C of the observations.

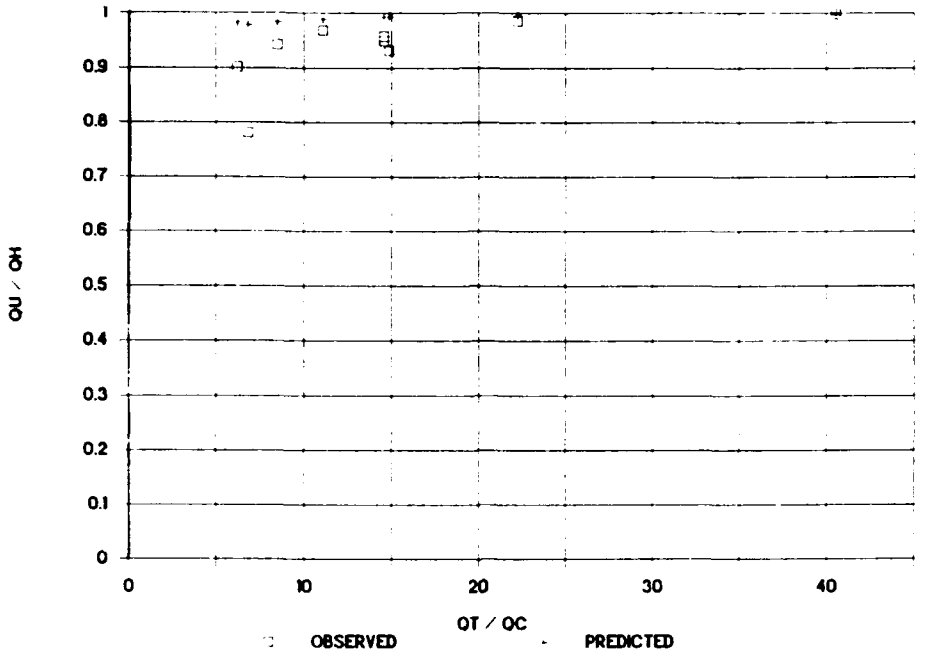

Figure 29. Predictions and observations from the Applegate Dam field study

All tests were conducted with the same stratification, the same two ports, and roughly the same total discharge. Therefore, the variation in release temperature from 10.5° C to over 16° C in Figure 30 arose almost entirely from throttling the intake ports.

139. The Elk Creek model is a 1:20-scale, Plexiglas representation of the proposed structure and the near-field topography. The prototype structure, once completed, will be about 73 m tall. Eight 1.52-m wide by 3.05-m tall water quality intake ports will enter a single wet well, 6.40 m wide by 2.13 m deep, in pairs at four invert elevations: 475.5, 490.7, 501.4, and 515.1 m. Each intake gate will be individually operable and capable of throttling.

140. For the model tests, salinity was again used to produce density stratifications analogous to those resulting from thermal stratification in the prototype reservoir. A wide range of stratification conditions were examined. The design flow range for the prototype was from 0.42 to 14.16 m^3/sec. The documentation of the model study conducted by Howington (in preparation) gives details of the testing procedures. Port flows were computed from the release information and from a model-verified, site-specific, selective-withdrawal description that provided the density entering each of the ports.

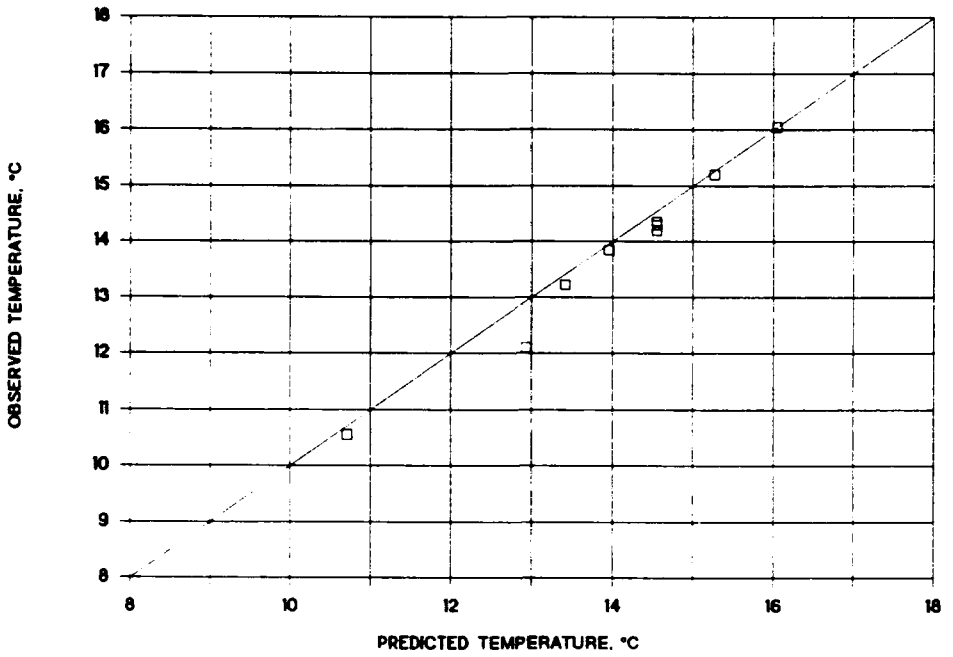

Figure 30. Predicted versus observed release temperatures for Applegate Dam

The buoyancy head, also dependent on the port densities, was computed as in Equation 39.

141. Head-loss coefficients, determined to be a function of gate opening, were computed in the model from direct measurement of the water surface differential from the pool to the wet well.

142. Comparisons between the SFD algorithm predictions and the physical-model observations are shown in Figure 31. Again, the predictions did not fall along a single curve since the head losses and areas among the ports were not identical (i.e., Equation 46 was applicable). However, it can be seen in the figure that the predictions and observations were generally close. A standard error of estimate of 7.8 percent in predicting the upper port flow contribution resulted from this comparison.

143. Many of the significant errors occurred very near critical discharge as was seen in previous comparisons. Two observations demonstrated a novel error in which the upper port flow was observed to be zero and predicted to be positive. These errors could be the result of overestimation of the loss coefficients. The large errors observed at high flows are attributable to errors in conductivity measurement during the determination of release density. The conductivity probes used are subject to corrosion problems in

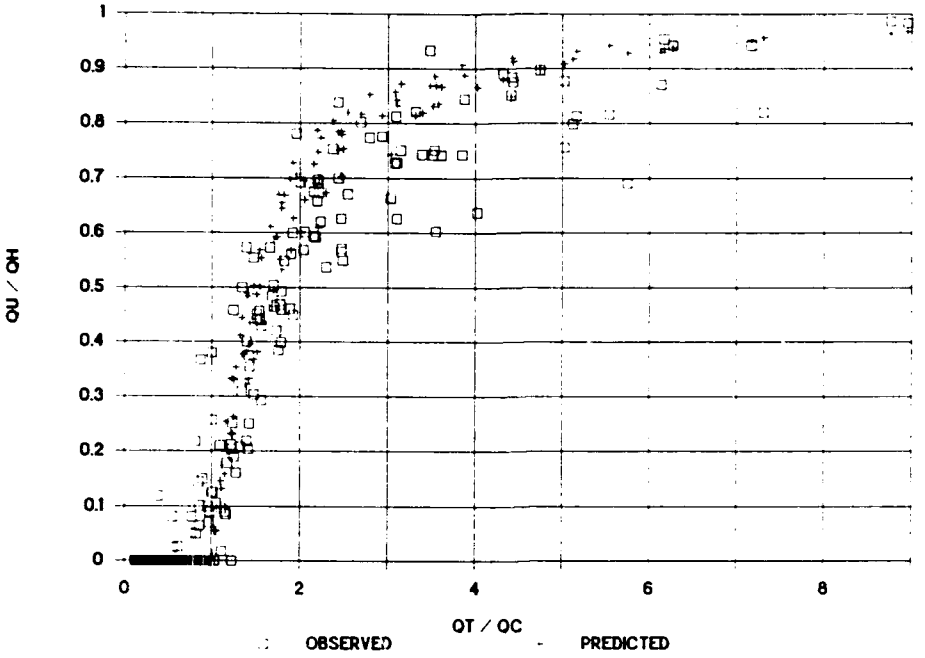

Figure 31. Predictions and observations from the Elk Creek model

saline water. Since the release density was used to determine port flows and the tests were conducted sequentially from low-to-high flows, some flow-observation errors were anticipated for the higher flows. The impacts of density were shown to diminish and become almost insignificant for discharges above 6 times the critical discharge.

Multiple-Wet-Well Structures

144. Although several single-flow-control, multiple-wet-well structures exist in the CE (Beltzville, Ray Roberts, and Gathright, for example), few observations are available during which both wells were operated during significant stratification. Therefore, data were collected in the laboratory.

145. A laboratory experiment was set up to exaggerate the differences between the single-well and multiple-well computation of the buoyancy head. The multiple-well computation includes the density difference between the two wells multiplied by the distance between the lowest operating port and the juncture of the release conduits (Equation 42). The test configuration shown in Figure 32 was used to verify Equation 42.

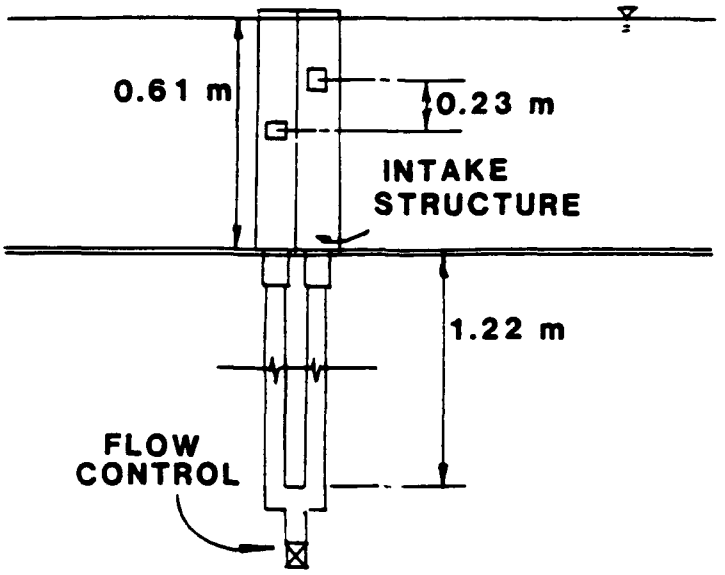

Figure 32. Multiple-well laboratory test situation

146. The scale-model structure was tested in a two-layer stratification. The wells were 0.091-m wide by 0.36-m deep; their height was 0.61 m. Flows from the two wells met where the release conduits joined, 1.2 m beneath the model. This configuration is similar to that for single flow control on a normally dual-flow-control, dual-wet-well system.

147. The intakes were 0.05-m wide by 0.043-m tall and were fully open. The range of flows was limited to those near the predicted critical discharge to maximize the effects of the buoyancy head and to determine whether the same errors encountered in previous comparisons would be encountered in two wells. Stratification was maintained through salinity. Head-loss coefficients were obtained by using a single piezometer to measure pressure at the juncture of the release conduits. The higher port flow was then computed using Equation 44; the predictions and observations are shown in Figure 33.

148. The SFD algorithm generally predicted closely the amount of flow passing through the higher port. The effects of density for the same ports and port elevations in a single wet well would have been much smaller since the port center lines were only 0.23 m apart in the model, indicating that the location where the waters meet in the wet well is important.

149. Also noteworthy is the absence of substantial errors near critical discharge. This absence of errors supports the proposition that the lower

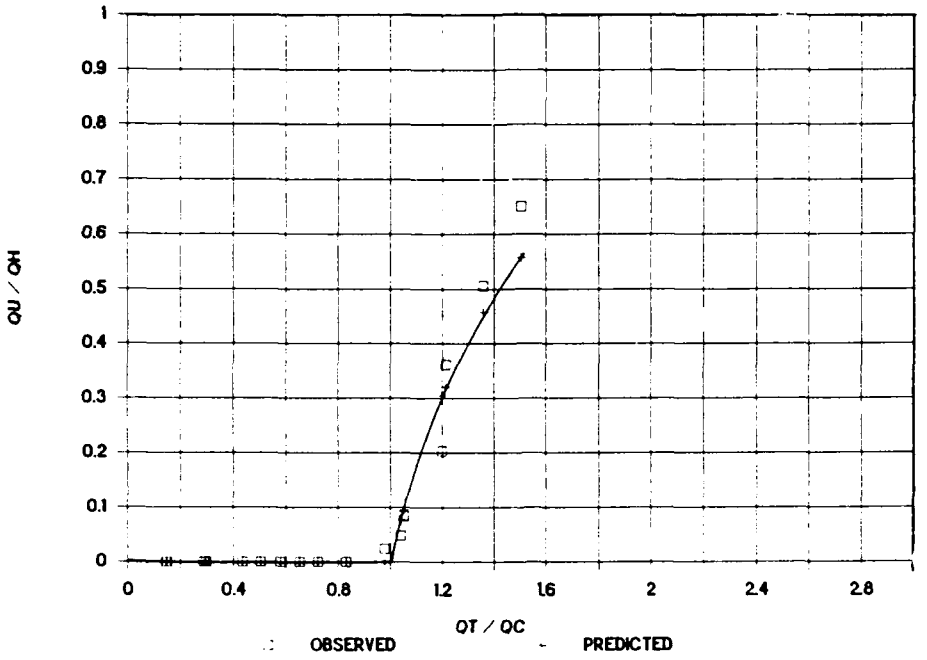

Figure 33. Predictions and observations for the multiple-well tests in a two-layer stratification

port velocity jet may be the consistent cause of the errors in the single-wet-well comparisons previously discussed since, in this case, the velocity jets enter individual wells. The only errors of significance here are at the higher flow rates. These were probably the result of withdrawal zones expanding into the layer not containing the port, which altered the densities entering each port.

General Notes on Comparability

150. The SFD algorithm has been tested for a wide variety of structures, stratifications, and port configurations. The comparisons with observed data have shown very good agreement except for a limited and well-defined range of conditions in a narrow band of discharges on either side of critical discharge. These discharges could be avoided in operation or, if necessary, described empirically on a site-specific basis.

151. An important consideration in the SFD algorithm is that the head losses must be known in advance to permit the flow distributions to be predicted correctly. The loss coefficients used herein have included the contraction/expansion losses as well as the in-structure losses. Estimation

of these coefficients in general may be difficult and may necessitate the use of a hydraulic model study or a prototype testing effort.

PART VI: APPLICATION TO OPERATIONS

152. The SFD algorithm for simultaneous, multiple-level withdrawal through a single flow control has been found to predict adequately the flow distribution among open ports, given the appropriate input. To effectively employ this extension of withdrawal technology, it has been incorporated into the SELECT model (Davis et al. 1987), the CE's standard model of selective withdrawal, which contains a subroutine for determining the best daily operations to achieve a desired release characteristic in a dual-wet-well, dual-flow-control system. This routine is based on the premise that the desired, stratified characteristic (often temperature) in the reservoir can often be obtained by blending flows from two ports, one in each wet well. The computer program calculates the flow requirements for each port. The influence of density on flow distribution for dual-flow-control systems is absent because independent flow controls are assumed to exist in the current SELECT version.

153. To provide a similar capability for single-flow-control structures, additional subroutines have been installed in SELECT. Two avenues were considered. If the intake ports can be throttled, an approach similar to the existing decision routine for port operation is employed. If the ports are operated fully open or fully closed, an alternate scheme is used.

154. If throttling is possible, the existing decision routine in SELECT is used to output the desired flow through each of two ports. This information is fed to a new routine that determines the gate settings required to produce the desired flow distribution. If this distribution cannot be achieved because of some physical constraint such as gate throttling limitations or velocity criteria, the single port that will best approximate the desired release characteristic is chosen. Iteration is often necessary in calculation of gate opening, because the dependence of the head-loss coefficients on the gate opening may be nonlinear. The head-loss equations for particular structures are presently entered directly into the code.

155. In a structure with more than two ports, none of which accommodate throttling, it is not known a priori which port combination will best provide the target release characteristics. Therefore, a general search routine was constructed that tests every possible combination of port openings allowed by the submergence and flow criteria. This routine computes the port flows and the release characteristics, compares them to the release target, and retains the best port combination. In a structure with many ports, such as Lost

Creek, criteria regarding the number of open ports for the specified total discharge were needed to limit the range of the search. With 12 intake ports from which to choose, the number of possible combinations would exceed 1,000.

156. Both the SELECT code and the modified SELECT code, including the SFD algorithm, run on personal computers or minicomputers. Run-times on personal computers are on the order of a few minutes for the throttling cases and are dependent on the number of ports for the no-throttling cases. The input requirements for the modified code are the same as the original SELECT model (a temperature or density profile, port geometries and elevations, maximum and minimum port flow criteria, release temperature target, site-specific withdrawal coefficients, and total discharge) except that head-loss coefficients must be furnished.

157. The short run-times with this code make it practical for both daily operations decisions as a stand-alone model and for operations forecasting when coupled with numerical reservoir models.

PART VII: SUMMARY AND CONCLUSIONS

Summary

158. Hydropower proliferation, increasing construction costs, and the evolution of environmental regulations have created a growing need for simultaneous, multiple-level withdrawal from a stratified reservoir through a single flow control. The ability to predict the density effects on flow distribution between multiple port elevations having the same flow control is thereby required. A method was desired that would produce reasonably accurate predictions and that could be easily transported and quickly applied among a wide array of structure designs. The technique to accomplish this should necessarily be simple and should avoid site specificity as much as possible.

159. An analytic approach has been developed using the Euler equation, beginning with simple cases and progressing to more complex problems. The resulting SFD algorithm predicts the flow distribution for any number of ports in an arbitrarily stratified fluid. This includes structures with wet-well outlets at any elevation.

160. The predictions of the algorithm have been compared with numerous observed data from the laboratory and the field, which include large and small wet-well structures, tall and short structures, gated and ungated structures, and single- and dual-well structures. The data encompass many unusual designs and many different flow rates and stratification conditions.

Conclusions

161. Simultaneous, multiple-level withdrawal from a density-stratified reservoir is viable, and the analytically based SFD algorithm adequately predicts flow distribution among multiple open ports. Density effects on the flow distribution are often significant, but they are stable, repeatable, and, in general, predictable.

162. For single-wet-well flows near critical discharge (the algorithm-predicted discharge required to overcome buoyancy blockage of one or more open ports), the algorithm underpredicts the upper port contribution to the total discharge. This underprediction may be caused by the velocity jet entering the lower port, since it does not occur for a two-well structure (Figure 33).

163. Operation in the range of discharges near critical discharge is generally undesirable since it is inherently unstable and provides little blending of the various water qualities. However, if flows near critical discharge were important for the operation of a particular intake structure, an empirical technique would probably have to be developed to predict the distribution of these flows.

164. Moreover, operation near critical discharge can be avoided by port throttling, which reduces the critical discharge significantly, thus placing a discharge that was previously in an unpredictable discharge region into one that is considerably more predictable.

165. For total discharges approximately 30 percent greater than critical or larger, the algorithm predicts the correct distribution to within less than 10 percent. For a two-ported structure with 20° C water entering the upper port and 4° C water entering the lower port, this error would correspond to a 1.6° C error in release temperature prediction.

166. For total discharges 5 or 6 times greater than the critical, the effects of density are far overshadowed by head losses. In the latter case, the flow distribution approaches that for homogeneous density.

167. Design of future single- or dual-wet-well reservoir intake structures should include serious consideration of port-throttling capabilities. This was shown to provide considerable control over the flow distribution among multiple open ports upstream of a single flow control.

REFERENCES

Bohan, J. P., and Gloriod, T. L. 1972. "Simultaneous, Multiple-Level Release from Stratified Reservoirs," Technical Report H-72-3, US Army Engineer Waterways Experiment Station, Vicksburg, MS.

Bohan, J. P., and Grace, J. L., Jr. 1969. "Mechanics of Flow from Stratified Reservoirs in the Interest of Water Quality; Hydraulics Laboratory Investigation," Technical Report H-69-10, US Army Engineer Waterways Experiment Station, Vicksburg, MS.

_____. 1973. "Selective Withdrawal from Man-Made Lakes; Hydraulic Laboratory Investigation," Technical Report H-73-4, US Army Engineer Waterways Experiment Station, Vicksburg, MS.

Brater, E. F., and King, H. W. 1976. Handbook of Hydraulics, McGraw-Hill, New York.

Callen, H. B. 1960. Thermodynamics, John Wiley and Sons, New York.

Cramer, S. P., Satterthwaite, T. D., Boyce, R. R., and McPherson, B. P. 1985. "Impacts of Lost Creek Dam on the Biology of Anadromous Salmonids in the Rogue River," Phase I Completion Report, Oregon Department of Fish and Wildlife, Portland, OR.

Craya, A. 1949. "Theoretical Research on the Flow of Superposed Layers of Fluids of Different Densities," La Houille Blanche, Vol 4, No. 1.

Croach, J. W. 1971. "Gravity Flow of a Stratified Fluid to a Sink," Report No. DP-1255, E. I. DuPont De Nemours and Co., Savannah River Laboratory, Aiken, SC.

Davis, J. E., Schneider, M. L., Holland, J. P., and Wilhelms, S. C. 1987. "SELECT: A Numerical, One-Dimensional Model for Selective Withdrawal," Instruction Report E-87-2, US Army Engineer Waterways Experiment Station, Vicksburg, MS.

Farrant, B. G. 1982. "Selective Withdrawal from a Linearly Stratified Reservoir," Master's Thesis, University of Canterbury, Christchurch, New Zealand.

Gariel, P. 1949. "Experimental Research on the Flow of Superposed Layers of Fluids of Different Densities," La Houille Blanche, Vol 4, No. 1.

Harleman, D. R. F., Morgan, R. L., and Purple, R. A. 1959. "Selective Withdrawal from a Vertically Stratified Fluid," Proceedings, 8th Congress, International Association for Hydraulic Research, Montreal.

Hino, M. 1980. "Discussion on Paper 'Selective Withdrawal: A Review' by J. Imberger and on Paper 'Selective Withdrawal Through a Point Sink' by G. A. Lawrence," Second International Symposium on Stratified Flows, Trondheim, Norway.

Hino, M., and Furusawa, M. 1969. "Experiments on Selective Withdrawal into a Sink from a Uniformly Stratified Fluid--Phenomenon of Layer Separation and Middle-Layer Withdrawal," Proceedings, 16th Japanese Conference on Coastal Engineering.

Howington, S. E. 1986. "Blending in a Single Wet Well," Proceedings: CE Workshop on Design and Operation of Selective Withdrawal Intake Structures, Miscellaneous Paper HL-86-3, US Army Engineer Waterways Experiment Station, Vicksburg, MS, pp 93-98.

_____. 1987. "Simultaneous Releases from a Stratified Reservoir," Proceedings of the 1987 National Conference on Hydraulic Engineering, R. M. Ragan, ed., American Society of Civil Engineers, New York, pp 42-47.

_____. 1988. "Multi-Ported, Single Wet-Well Intake Structure Operation in a Stratified Reservoir," Water Quality '88 Seminar Proceedings, US Army Corps of Engineers Committee on Water Quality, Washington, DC, pp 32-38.

_____. 1989. "Intake Structure Operation Study, Lost Creek Dam, Oregon," Technical Report HL-89-13, US Army Engineer Waterways Experiment Station, Vicksburg, MS.

_____. "Intake Structure Operation Study, Elk Creek Dam, Oregon," Technical Report in preparation, US Army Engineer Waterways Experiment Station, Vicksburg, MS.

Hutchinson, G. E. 1957. Treatise on Limnology; Vol I. Geography, Physics, and Chemistry, John Wiley and Sons, New York.

Kittrell, F. W. 1965. "Thermal Stratification in Reservoirs," Symposium on Streamflow Regulation for Quality Control, US Department of Health, Education, and Welfare, p 279.

Lagler, K. F. 1956. Freshwater Fishery Biology, William C. Brown Co., Dubuque, IA, pp 263-265.

Lawrence, G. A., and Imberger, J. 1979. "Selective Withdrawal Through a Point Sink in a Continuously Stratified Fluid with Pycnocline," Report No. ED-79-002, University of Western Australia, Nedland, Western Australia.

Miller, D. S. 1978. Internal Flow Systems, British Hydromechanics Research Association Fluid Engineering Series, Vol 5.

Smith, D. R., Wilhelms, S. C., Holland, J. P., Dortch, M. S., and Davis, J. E. 1987. "Improved Description of Selective Withdrawal Through Point Sinks," Technical Report E-87-2, US Army Engineer Waterways Experiment Station, Vicksburg, MS.

Steel, R. G. D., and Torrie, J. H. 1960. Principles and Procedures of Statistics, McGraw-Hill, New York.

Streeter, V. L., and Wylie, E. B. 1975. Fluid Mechanics, McGraw-Hill, New York, pp 110-133.

Thompson, P. A. 1972. Compressible-Fluid Dynamics, McGraw-Hill, New York, pp 15-16.

US Army, Office of the Chief of Engineers. 1968. Hydraulic Design Criteria, prepared by the US Army Engineer Waterways Experiment Station, Vicksburg, MS.

Vennard, J. K., and Street, R. L. 1975. Elementary Fluid Mechanics, John Wiley and Sons, New York, pp 379-463.

Wetzel, R. G. 1975. Limnology, W. B. Saunders Co., Philadelphia, pp 6-65.

APPENDIX A: EULER EQUATION

1. The derivation of the Euler equation used in this study closely follows that in Streeter and Wylie (1975).*

2. Consider a control volume in a velocity field. Let N(t) be the amount of a given property in the control volume at time t. Also let η be a function describing the amount of this property per unit mass throughout the fluid. Therefore, by the Reynolds' transport theorem (Thompson 1972), the change in N within the control volume with respect to time can be written as

$$\frac{dN}{dt} = \int_{cv} \eta \frac{\partial \rho}{\partial t} dU + \int_{cs} \eta \rho \vec{V} \cdot d\vec{A} \qquad \text{(A1)}$$

where

cv = control volume

ρ = mass density of the fluid

dU = incremental volume in the control volume

cs = the surface of the control volume

$\vec{V}$ = velocity vector in the velocity field

$d\vec{A}$ = incremental area on the surface of the control volume

3. Also, consider the first law of thermodynamics (Callen 1960), which states that the incremental heat added to a system (ΔQ) minus the incremental work (ΔW) done by a system depends only on the initial and final internal energy states of the system, defined as E and $E + \Delta E$, respectively. In equation form, this is

$$\frac{\Delta Q - \Delta W}{\Delta t} = \frac{\Delta E}{\Delta t} \qquad \text{(A2)}$$

4. The work term can be decomposed into shaft and pressure work. The pressure work can be described by

---

* See References at the end of the main text.

$$\frac{\Delta W_{pr}}{\Delta t} = \int_{cs} p\mathbf{V} \cdot d\mathbf{A} \tag{A3}$$

5. Applying Equation A1 with the property N as internal energy and e as internal energy per unit mass gives

$$\frac{dN}{dt} = \int_{cv} e \frac{\partial \rho}{\partial t} dU + \int_{cs} e\rho \mathbf{V} \cdot d\mathbf{A} \tag{A4}$$

Combining Equations A2 through A4 produces

$$\frac{\Delta Q}{\Delta t} - \frac{\Delta W}{\Delta t} = \int_{cv} e \frac{\partial \rho}{\partial t} dU + \int_{cs} \left(\frac{p}{\rho} + e\right) \rho \mathbf{V} \cdot d\mathbf{A} \tag{A5}$$

with the internal energy e being $gz + v^2/2 + u$, where u is the intrinsic energy resulting from molecular spacing and forces.

6. When Equation A5 is applied to steady, incompressible flow through a control volume, the first term on the right side of Equation A5 goes to zero. The result is

$$\frac{\Delta Q}{\Delta t} - \frac{\Delta W}{\Delta t} = \left(\frac{p_2}{\rho_2} + gz_2 + \frac{v_2^2}{2} + u_2\right) \rho_2 v_2 A_2 - \left(\frac{p_1}{\rho_1} + gz_1 + \frac{v_1^2}{2} + u_1\right) \rho_1 v_1 A_1 \tag{A6}$$

where the subscripts 1 and 2 refer to the inflow and outflow boundaries of the control volume, respectively. For steady flow, $\rho_2 v_2 A_2 = \rho_1 v_1 A_1$. If Equation A6 is divided by the mass flow per second, the heat added, and shaft work are expressed per unit mass of the fluid (q and w_s, respectively), the following equation results

$$q + \frac{p_1}{\rho_1} + gz_1 + \frac{v_1^2}{2} + u_1 = w_s + \frac{p_2}{\rho_2} + gz_2 + \frac{v_2^2}{2} + u_2 \tag{A7}$$

7. When applied through a stream tube with no shaft work, this equation, expressed in differential form, becomes

$$\frac{dp}{\rho} + gdz + vdv + du + pd\frac{1}{\rho} - dq = 0 \qquad \text{(A8)}$$

From the first law of thermodynamics and the definition of entropy (s)

$$Tds = pd\frac{1}{\rho} + du \qquad \text{(A9)}$$

where T is the absolute temperature. Substituting into Equation A8 produces

$$\frac{dp}{\rho} + gdz + vdv + Tds - dq = 0 \qquad \text{(A10)}$$

By the definition of an irreversible process,

$$Tds \geq dq \qquad \text{(A11)}$$

8. If losses (or irreversible changes) are identified by

$$d(losses) = Tds - dq \qquad \text{(A12)}$$

then, by substituting Equation A12 into Equation A10 and applying it between points 1 and 2, the following is produced:

$$\frac{v_1^2}{2} + gz_1 = \int_1^2 \frac{dp}{\rho} + \frac{v_2^2}{2} + gz_2 + losses_{1-2} \qquad \text{(A13)}$$

Equation A13, with the exception of the loss term, is the integral Euler equation.